A Least-Squares Monte Carlo Approach to the Calculation of Capital Requirements*

Hongjun Ha

Department of Mathematics; Saint Joseph's University

5600 City Avenue, Philadelphia, PA 19131. USA

Daniel Bauer†

Department of Economics, Finance, and Legal Studies; University of Alabama

361 Stadium Drive, Tuscaloosa, AL 35486. USA

First version: September 2013. This version: February 2018.

Abstract

The calculation of capital requirements for financial institutions entails a reevaluation of the company's assets and liabilities at some future point in time for a (large) number of stochastic forecasts of economic and firm-specific variables. Relying on well-known ideas for pricing non-European derivatives, the current paper discusses tackling this *nested* valuation problem based on Monte Carlo simulations and least-squares regression techniques. We study convergence of the algorithm and analyze the resulting estimate for practically relevant risk measures. Importantly, we address the problem of how to choose the regressors ("basis functions"), and show that an optimal choice is given by the left singular functions of the corresponding conditional expectation operator. Our numerical examples demonstrate that the algorithm can produce accurate results at relatively low computational costs, particularly when relying on the optimal basis functions.

Keywords: capital requirements, least-squares Monte Carlo, Value-at-Risk, singular value decomposition, regularized regression, Variable Annuity with GMB.

*This paper extends an earlier working paper Bauer et al. (2010). We thank Giuseppe Benedetti, Enrico Biffis, René Carmona, Matthias Fahrenwaldt, Jean-Pierre Fouque, Andreas Reuss, Daniela Singer, Ajay Subramanian, Baozhong Yang, and seminar participants at the Bachelier Congress 2014, the World Risk and Insurance Economics Congress 2015, the 2017 Conference Innovations in Insurance Risk and Asset Management at TU Munich, the 2017 Conference for the 10th Anniversary of the Center for Financial Mathematics and Actuarial Research at USCB, Georgia State University, Michigan State University, St. Joseph's University, Université de Montréal, and Barrie & Hibbert for helpful comments. The usual disclaimer applies.

†Corresponding author. Phone: +1-205-348-8486. E-mail addresses: hha@sju.edu (H. Ha); dbauer@cba.ua.edu (D. Bauer).

1 Introduction

Many financial risk management applications entail a reevaluation of the company's assets and liabilities at some time horizon τ – sometimes called a *risk horizon* – for a large number of realizations of economic and firm-specific (state) variables. The resulting empirical loss distribution is then applied to derive risk measures such as Value-at-Risk (VaR) or Expected Shortfall (ES), which serve as the basis for capital requirements within several regulatory frameworks such as Basel III for banks and Solvency II for insurance companies. However, the high complexity of this *nested* computation structure leads firms to struggle with the implementation.

This paper discusses an approach to this problem based on least-squares regression and Monte Carlo simulations akin to the well-known Least-Squares Monte Carlo method (LSM) for pricing non-European derivatives introduced by Longstaff and Schwartz (2001). Analogously to the LSM pricing method, this approach relies on two approximations (Clément et al., 2002): On the one hand, the capital random variable, which can be represented as a risk-neutral conditional expected value at the risk horizon τ, is replaced by a finite linear combination of functions of the state variables, so-called *basis functions*. As the second approximation, Monte Carlo simulations and least-squares regression are employed to estimate the coefficients in this linear combination. Hence, for each realization of the state variables, the resulting linear combination presents an approximate realization of the capital at τ, and the resulting sample can be used for estimating relevant risk measures.

Although this approach is increasingly popular in practice for calculating economic capital particularly in the insurance industry (Barrie and Hibbert, 2011; Milliman, 2013; DAV, 2015) and has been used in several applied research contributions (Floryszczak et al., 2016; Pelsser and Schweizer, 2016, e.g.), these papers do not provide a detailed analysis of the properties of this algorithm or insights on how to choose the basis functions. Our work closes this gap in literature.

We begin our analysis by introducing our setting and the algorithm. As an important innovation, we frame the estimation problem via a *valuation operator* that maps future payoffs (as functionals of the state variables) to the conditional expected value at the risk horizon. We formally establish convergence of the algorithm for the risk distribution (in probability) and for families of risk measures under general conditions when taking limits sequentially in the first and second approximation. In addition, by relying on results from Newey (1997) on the convergence of series estimators, we present conditions for the joint convergence of the two approximations in the general case and more explicit results for the practically relevant case of orthonormal polynomials.

We then analyze in more detail the properties of the estimator for the important special case of VaR, which serves as the risk measure for regulatory frameworks such as Solvency II. By building on ideas from Gordy and Juneja (2010), we show that for a fixed number of basis functions, the least-squares estimation of the regression approximation, while unbiased when viewed as an estimator for the individual loss, carries a positive bias term for this tail risk measure. It is important to note, however, that this result only pertains to the regression approximation but not the approximation of the actual loss variables via the linear combination of the basis functions – which is the crux of the algorithm. In particular, the adequacy of the estimate crucially depends on the choice of basis functions.

This is where the operator formulation becomes especially useful. By expressing the valuation operator via its singular value decomposition (SVD), we show that under certain conditions, the (left) singular functions present an optimal choice for the basis functions. More precisely, we demonstrate that these singular functions approximate the valuation operator – and, thus, the distribution of relevant capital levels – in an optimal manner. The intuition is that similarly to an SVD for a matrix, the singular functions provide the most important dimensions in spanning the image space of the operator.

We comment on the joint convergence of the LSM algorithm under this choice and also the calculation of the singular functions. While in general the decomposition has to be carried out numerically, for certain classes of models it is possible to derive analytic expressions. As an important example class for applications, we discuss the calculation of the SVD – and, thus, the derivation of optimal basis functions – for models with (multivariate) Gaussian transition densities. In this case, it is straightforward to show that the underlying assumptions are satisfied. And, by following ideas from Khare and Zhou (2009), it is possible to derive the singular functions, which take the form of products of Hermite polynomials of linearly transformed states, by solving a related eigenvalue problem. We note that, in analogy to e.g. Discriminant Analysis, these results will also be useful in non-Gaussian settings by proposing approximately optimal basis functions that solely rely on the first two moments of the state vector distribution.

We illustrate our theoretical results considering popular annuitization guarantees within Variable Annuity contracts, so-called Guaranteed Minimum Income Benefits (GMIBs). In a setting with three stochastic risk factors (investment fund, interest, and mortality), we demonstrate that the algorithm delivers reliable results when relying on sufficiently many basis functions and simulations. Here we emphasize that the optimal choice given by the singular functions not only determines the functional class – which are Hermite polynomials in this case, although of course different classes of univariate polynomials will generate the same span. But they also specify the most important combinations of stochastic factors, an indeed in our setting it turns out that higher-order combinations of certain risk factors are more important than lower-order combinations of others. This latter aspect is very relevant in practical settings with high-dimensional state vectors, so that our results provide immediate guidance for these pressing problems. We also illustrate the tradeoff between sample variance – governed by the number of considered scenarios – and the functional approximation – depending on the number of considered basis functions. We document that navigating this tradeoff is important for obtaining viable results, and doing so is nontrivial in general. In particular, we comment on pitfalls when using regularized regression approaches in this context.

Related Literature and Organization of the Paper

Our approach is inspired by the LSM approach for derivative pricing and relies on corresponding results (Carriere, 1996; Tsitsiklis and Van Roy, 2001; Longstaff and Schwartz, 2001; Clément et al., 2002). A similar regression-based algorithm for risk estimation is independently studied in Broadie et al. (2015). Their results are similar to our sequential convergence results in Section 3.1, and the authors additionally introduce a *weighted* version of their regression algorithm. Moreover, Benedetti (2017) provides joint convergence results

under an alternative set of conditions. However, these authors do not contemplate how to optimally choose the basis functions – although they emphasize the importance of this choice – which is a key contribution of our paper.

We refer to Makur and Zheng (2016) for the relevance of the SVD of conditional expectations in the information theory literature, which is driven by similar considerations. In particular, the authors derive the analogous SVD for the Gaussian setting in the univariate case (see also Abbe and Zheng (2012)). The relevance of Hermite polynomials in this context may not come as a surprise from a stochastic process perspective due to their relevance in the spectral analysis of the Ornstein-Uhlenbeck semigroup (Linetsky, 2004). However, as detailed in Makur and Zheng (2016, p. 636), we note that the setting here is distinct from Markov semigroup theory, where the relevant spaces are framed in terms of invariant measures and the time interval varies.

As already indicated, the LSM approach enjoys popularity in the context of calculating risk capital for life insurance liabilities in practice and applied research, so that providing a theoretical foundation and guidance for its application are key motivating factors for this paper. A number of recent contributions discuss the so-called *replicating portfolio approach* as an alternative that enjoys certain advantages (Cambou and Filipović, 2018; Natolski and Werner, 2017, e.g.), and Pelsser and Schweizer (2016) point out that the difference between the LSM versus the replicating portfolio calculation aligns with the so-called *regression-now* versus the so-called *regression-later* algorithm, respectively, for non-European option pricing (Glasserman and Yu, 2002). While a detailed comparison is beyond the scope of this paper, we note that although indeed in simple settings the performance of regress-later approaches appears superior (Beutner et al., 2013), the application comes with several caveats regarding the existence of suitable financial securities, the choice of the basis functions, and other complications in high-dimensional settings (Pelsser and Schweizer, 2016; Ha, 2016).

Another set of recent papers propose non-parametric smoothing approaches in the nested simulations context, e.g. by relying on Gaussian process emulation ("kriging") or kernel smoothing (Liu and Staum, 2010; Chen et al., 2012; Hong et al., 2017; Risk and Ludkovski, 2017). In addition to the benefit of relative simplicity of LSM in practical applications, the non-parametric approaches may also suffer from limitations in high-dimensional settings due to the curse of dimensionality. Indeed, Hong et al. (2017) show that already starting in five dimensions, the convergence properties of a basic nested simulations estimator can be superior. This is particularly relevant in the insurance context that we have in our focus, since problems are usually high-dimensional and it generally is not possible to decompose enterprise-wide risk measurement into lower dimensional problems (Hong et al., 2017) due to the relevance of firm specific variables for all contracts. However, as pointed out by Risk and Ludkovski (2017, Sec. 5.3), integrating regression-based approaches as considered here with emulation techniques presents a promising avenue for future research. Similarly, tailoring our approach to the evaluation of specific risk measures, e.g. those that focus on the tail of the distribution such as VaR and ES following ideas of Glasserman et al. (2000), Lan et al. (2010), and Broadie et al. (2011), presents an interesting question left for future research.

The remainder of the paper is structured as follows: Section 2 lays out the simulation framework and the algorithm; Section 3 addresses convergence of the algorithm and analyzes the estimator in special cases; Section 4 discusses optimal basis functions and derives them in models with Gaussian transition densities; Section 5 provides our numerical example; and,

finally, Section 6 concludes. Proofs and technical details are relegated to the Appendix.

2 The LSM Approach

2.1 Simulation Framework

Let $(\Omega, \mathcal{F}, \mathbf{F} = (\mathcal{F}_t)_{t\in[0,T]}, \mathbb{P})$ be a complete filtered probability space on which all relevant quantities exist, where T corresponds to the longest-term asset or liability of the company in view and $\mathbb{P}$ denotes the physical measure. We assume that all random variables in what follows are square-integrable (in $L^2(\Omega, \mathcal{F}, \mathbb{P})$). The sigma algebra $\mathcal{F}_t$ represents all information up to time t, and the filtration $\mathbf{F}$ is assumed to satisfy the usual conditions.

The uncertainty with respect to the company's future assets and liabilities arises from the uncertain development of a number of influencing factors, such as equity returns, interest rates, demographic or loss indices, etc. We introduce the d-dimensional, sufficiently regular Markov process $Y = (Y_t)_{t\in[0,T]} = (Y_{t,1}, \ldots, Y_{t,d})_{t\in[0,T]}$, $d \in \mathbb{N}$, the so-called *state process*, to model this uncertainty. We assume that all financial assets in the market can be expressed in terms of Y. Non-financial risk factors can also be incorporated (see e.g. Zhu and Bauer (2011) for a life insurance setting that includes demographic risk). In this market, we take for granted the existence of a risk-neutral probability measure (martingale measure) $\mathbb{Q}$ equivalent to $\mathbb{P}$ under which payment streams can be valued as expected discounted cash flows with respect to a given numéraire process $(N_t)_{t\in[0,T]}$.

In financial risk management, we are now concerned with the company's financial situation at a certain (future) point in time τ, $0 < \tau < T$, which we refer to as the *risk horizon*. More specifically, based on realizations of the state process Y over the time period $[0, \tau]$ that are generated under the physical measure $\mathbb{P}$, we need to assess the *available capital* C_τ at time τ calculated as the market value of assets minus liabilities. This amount can serve as a buffer against risks and absorb financial losses. The *capital requirement* is then defined via a risk-measure ρ applied to the capital random variable. For instance, if the capital requirement is cast based on VaR, the capitalization at time τ should be sufficient to cover the net liabilities at least with a probability α, i.e. the additionally required capital is:

$$\mathrm{VaR}_\alpha(-C_\tau) = \inf\left\{ x \in \mathbb{R} \middle| \, \mathbb{P}\left(x + C_\tau \geq 0\right) \geq \alpha \right\}. \tag{1}$$

The capital at the risk horizon, for each realization of the state process Y, is derived from a market-consistent valuation approach. While the market value of traded instruments is usually readily available from the model ("mark-to-market"), the valuation of complex financial positions on the firm's asset side such as portfolios of derivatives and/or the valuation of complex liabilities such as insurance contracts containing embedded options typically require numerical approaches. This is the main source of complexity associated with this task, since the valuation needs to be carried out for each realization of the process Y at time τ, i.e. we face a *nested* valuation problem.

Formally, the available capital is derived as a (risk-neutral) conditional expected value of discounted cash flows X_t, where for simplicity and to be closer to modeling practice, we

assume that cash flows only occur at discrete times $t = 1, 2, \ldots, T$ and that $\tau \in \{1, 2, \ldots, T\}$:

$$C_\tau = \mathbb{E}^{\mathbb{Q}} \left[\sum_{k=\tau}^{T} \frac{N_\tau}{N_k} X_k \middle| (Y_s)_{0 \le s \le \tau} \right]. \tag{2}$$

Note that within this formulation, interim asset and liability cash flows in $[0, \tau]$ may be aggregated in the $\sigma(Y_s, 0 \le s \le \tau)$-measurable position X_τ. Moreover, in contrast to e.g. Gordy and Juneja (2010), we consider aggregate asset and liability cash flows at times $k \ge \tau$ rather than cash flows corresponding to individual asset and liability positions. Aside from notational simplicity, the reason for this formulation is that we particularly focus on situations where an independent evaluation of many different positions is not advisable or feasible as it is for instance the case within economic capital modeling in life insurance (Bauer et al., 2012b).

In addition to current interest rates, security prices, etc., the value of the asset and liability positions may also depend on path-dependent quantities. For instance, Asian options depend on the average of a certain price index over a fixed time interval, lookback options depend on the running maximum, and liability values in insurance with profit sharing mechanisms depend on entries in the insurer's bookkeeping system. In what follows, we assume that – if necessary – the state process Y is augmented so that it contains all quantities relevant for the evaluation of the available capital and still satisfies the Markov property (Whitt, 1986). Thus, we can write:

$$C_\tau = \mathbb{E}^{\mathbb{Q}} \left[\sum_{k=\tau}^{T} \frac{N_\tau}{N_k} X_k \middle| Y_\tau \right].$$

We refer to the state process Y as our *model framework*. Within this *framework*, the asset-liability projection *model* of the company is given by cash flow projections of the asset-liability positions, i.e. functionals x_k that derive the cash flows X_k based on the current state Y_k:[1]

$$\frac{N_\tau}{N_k} X_k = x_k (Y_k), \ \tau \le k \le T.$$

Hence, each *model* within our *model framework* can be identified with an element in a suitable function space, $\mathbf{x} = (x_\tau, x_{\tau+1}, ..., x_T)$. More specifically, we can represent:

$$C_\tau (Y_\tau) = \sum_{j=\tau}^{T} \mathbb{E}^{\mathbb{Q}} \left[x_j (Y_j) \middle| Y_\tau \right].$$

We now introduce the probability measure $\tilde{\mathbb{P}}$ via its Radon-Nikodym derivative:

$$\frac{\partial \tilde{\mathbb{P}}}{\partial \mathbb{P}} = \frac{\frac{\partial \mathbb{Q}}{\partial \mathbb{P}}}{\mathbb{E}^{\mathbb{P}} \left[\frac{\partial \mathbb{Q}}{\partial \mathbb{P}} | \mathcal{F}_\tau \right]}.$$

[1] Similarly to Section 8.1 in Glasserman (2004), without loss of generality, by possibly augmenting the state space or by changing the numéraire process (see Section 5), we assume that the discount factor can be expressed as a function of the state variables.

Lemma 2.1. *We have:*

1. $\tilde{\mathbb{P}}(A) = \mathbb{P}(A),\ A \in \mathcal{F}_t,\ 0 \leq t \leq \tau$.
2. $\mathbb{E}^{\tilde{\mathbb{P}}}[X|\,\mathcal{F}_\tau] = \mathbb{E}^{\mathbb{Q}}[X|\,\mathcal{F}_\tau]$ *for every random variable* $X \in \mathcal{F}$.

Lemma 2.1 implies that we have:

$$C_\tau(Y_\tau) \;=\; \sum_{j=\tau}^{T} \mathbb{E}^{\tilde{\mathbb{P}}}[x_j(Y_j)|\,Y_\tau] = L\,\mathbf{x}(Y_\tau), \tag{3}$$

where the operator:

$$L : \mathcal{H} = \bigoplus_{j=\tau}^{T} L^2(\mathbb{R}^d, \mathcal{B}, \tilde{\mathbb{P}}_{Y_j}) \to L^2(\mathbb{R}^d, \mathcal{B}, \mathbb{P}_{Y_\tau}) \tag{4}$$

is mapping a model to capital. We call L in (4) the *valuation operator*. For our applications later in the text, it is important to note the following:

Lemma 2.2. *L is a continuous linear operator.*

Moreover, for our results on the optimality of basis functions, we require compactness of the operator L. The following lemma provides a version of the well-known Hilbert-Schmidt condition for L to be compact in terms of the transition densities (Breiman and Friedman, 1985):

Lemma 2.3. *Assume there exists a joint density $\pi_{Y_\tau,Y_j}(y,x)$, $j = \tau, \tau+1, ..., T$, for Y_τ and Y_j. Moreover:*

$$\int_{\mathbb{R}^d}\int_{\mathbb{R}^d} \pi_{Y_j|Y_\tau}(y|x)\,\pi_{Y_\tau|Y_j}(x|y)\,dy\,dx < \infty,$$

where $\pi_{Y_j|Y_\tau}(y|x)$ and $\pi_{Y_\tau|Y_j}(x|y)$ denote the transition density and the reverse transition density, respectively. Then the operator L is compact.

The definition of L implies that a model can be identified with an element of the Hilbert space $\mathcal{H}$ whereas (state-dependent) capital C_τ can be identified with an element of $L^2(\mathbb{R}^d, \mathcal{B}, \mathbb{P}_{Y_\tau})$. The task at hand is now to evaluate this element for a given model $\mathbf{x} = (x_\tau, \ldots, x_T)$ and to then determine the capital requirement via a (monetary) risk measure $\rho : L^2(\mathbb{R}^d, \mathcal{B}, \mathbb{P}_{Y_\tau}) \to \mathbb{R}$ as $\rho(L\mathbf{x})$, although the *model* may change between applications as the exposures may change (e.g. from one year to the next or when evaluating capital allocations via the gradient of ρ (Bauer and Zanjani, 2016)).

One possibility to carry out this computational problem is to rely on *nested simulations*, i.e. to simulate a large number of scenarios for Y_τ under $\mathbb{P}$ and then, for each of these realizations, to determine the available capital using another simulation step under $\mathbb{Q}$. The resulting (empirical) distribution can then be employed to calculate risk measures (Lee, 1998; Gordy and Juneja, 2010). However, this approach is computationally burdensome and, for some relevant applications, may require a very large number of simulations to obtain results in a reliable range (Bauer et al., 2012b). Hence, in the following, we develop an alternative approach for such situations.

2.2 Least-Squares Monte-Carlo (LSM) Algorithm

As indicated in the previous section, the task at hand is to determine the distribution of C_τ given by Equation (3). Here, the conditional expectation causes the primary difficulty for developing a suitable Monte Carlo technique. This is akin to the pricing of Bermudan or American options, where "*the conditional expectations involved in the iterations of dynamic programming cause the main difficulty for the development of Monte-Carlo techniques*" (Clément et al., 2002). A solution to this problem was proposed by Carriere (1996), Tsitsiklis and Van Roy (2001), and Longstaff and Schwartz (2001), who use least-squares regression on a suitable finite set of functions in order to approximate the conditional expectation. In what follows, we exploit this analogy by transferring their ideas to our problem.

As pointed out by Clément et al. (2002), their approach consists of two different types of approximations. Proceeding analogously, as the first approximation, we replace the conditional expectation, C_τ, by a finite combination of linearly independent basis functions $e_k(Y_\tau) \in L^2\left(\mathbb{R}^d, \mathcal{B}, \mathbb{P}_{Y_\tau}\right)$:

$$C_\tau \approx \widehat{C}_\tau^{(M)}(Y_\tau) = \sum_{k=1}^{M} \alpha_k \cdot e_k(Y_\tau). \tag{5}$$

We then determine approximate $\mathbb{P}$-realizations of C_τ using Monte Carlo simulations. We generate N independent paths $(Y_t^{(1)})_{0\le t\le T}$, $(Y_t^{(2)})_{0\le t\le T}$,..., $(Y_t^{(N)})_{0\le t\le T}$, where we generate the Markovian increments under the physical measure for $t \in (0, \tau]$ and under the risk-neutral measure for $t \in (\tau, T]$.[2] Based on these paths, we calculate the realized cumulative discounted cash flows:

$$V_\tau^{(i)} = \sum_{j=\tau}^{T} x_j \left(Y_j^{(i)}\right),\ 1 \le i \le N.$$

We use these realizations in order to determine the coefficients $\alpha = (\alpha_1, \ldots, \alpha_M)$ in the approximation (5) by least-squares regression:

$$\hat{\alpha}^{(N)} = \text{argmin}_{\alpha\in\mathbb{R}^M} \left\{ \sum_{i=1}^{N} \left[V_\tau^{(i)} - \sum_{k=1}^{M} \alpha_k \cdot e_k\left(Y_\tau^{(i)}\right) \right]^2 \right\}.$$

Replacing α by $\hat{\alpha}^{(N)}$, we obtain the second approximation:

$$C_\tau \approx \widehat{C}_\tau^{(M)}(Y_\tau) \approx \widehat{C}_\tau^{(M,N)}(Y_\tau) = \sum_{k=1}^{M} \hat{\alpha}_k^{(N)} \cdot e_k(Y_\tau), \tag{6}$$

based on which we can then calculate $\rho\left(L\,\mathbf{x}\right) \approx \rho(\widehat{C}_\tau^{(M,N)})$.

In case the distribution of Y_τ, $\mathbb{P}_{Y_\tau}$, is not directly accessible, we can calculate realizations of $\widehat{C}_\tau^{(M,N)}$ resorting to the previously generated paths $(Y_t^{(i)})_{0\le t\le T}$, $i = 1, \ldots, N$, or, more

[2]Note that it is possible to allow for multiple *inner* simulations under the risk-neutral measure per *outer* simulation under $\mathbb{P}$ as in the algorithm proposed by Broadie et al. (2015). However, as shown in their paper, a single inner scenario as within our version will be the optimal choice when allocating a finite computational budget. The intuition is that the inner noise diversifies in the regression approach whereas additional outer scenarios add to the information regarding the relevant distribution.

precisely, to the sub-paths for $t \in [0, \tau]$. Based on these realizations, we can determine the corresponding empirical distribution function and, consequently, an estimate for $\rho(\widehat{C}_\tau^{(M,N)})$. For the analysis of potential errors when approximating the risk measure based on the empirical distribution function, we refer to Weber (2007).

3 Analysis of the Algorithm

3.1 Convergence

The following proposition establishes convergence of the algorithm described in Section 2.2 when taking limits sequentially:

Proposition 3.1. *$\widehat{C}_\tau^{(M)} \to C_\tau$ in $L^2(\mathbb{R}^d, \mathcal{B}, \mathbb{P}_{Y_\tau})$, $M \to \infty$, and $\widehat{C}_\tau^{(M,N)} \to \widehat{C}_\tau^{(M)}$, $N \to \infty$, $\tilde{\mathbb{P}}$-almost surely. Furthermore, $Z^{(N)} = \sqrt{N}\left[\widehat{C}_\tau^{(M)} - \widehat{C}_\tau^{(M,N)}\right] \longrightarrow$ Normal $(0, \xi^{(M)})$, where $\xi^{(M)}$ is provided in Equation (23) in the Appendix.*

We note that the proof of this convergence result is related to and simpler than the corresponding result for the Bermudan option pricing algorithm in Clément et al. (2002) since we do not have to take the recursive nature into account. The primary point of Proposition 3.1 is the convergence in probability – and, hence, in distribution – of $\widehat{C}_\tau^{(M,N)} \to C_\tau$ implying that the resulting distribution function of $\widehat{C}_\tau^{(M,N)}$ presents a valid approximation of the distribution of C_τ for large M and N. The question of whether $\rho(\widehat{C}_\tau^{(M,N)})$ presents a valid approximation of $\rho(C_\tau)$ depends on the regularity of the risk measure. In general, we require continuity in $L^2(\mathbb{R}^d, \mathcal{B}, \mathbb{P}_{Y_\tau})$ as well as point-wise continuity with respect to almost sure convergence (see Kaina and Rüschendorf (2009) for a corresponding discussion in the context of convex risk measures). In the special case of orthogonal basis functions, we are able to present a more concrete result:

Corollary 3.1. *If $\{e_k,\, k = 1, \ldots, M\}$ are orthonormal, then $\widehat{C}_\tau^{(M,N)} \to C_\tau$, $N \to \infty$, $M \to \infty$ in $L^1(\mathbb{R}^d, \mathcal{B}, \mathbb{P}_{Y_\tau})$. In particular, if ρ is a finite convex risk measure on $L^1(\mathbb{R}^d, \mathcal{B}, \mathbb{P}_{Y_\tau})$, we have $\rho(\widehat{C}_\tau^{(M,N)}) \to \rho\left(C_\tau\right)$, $N \to \infty$, $M \to \infty$.*

Thus, at least for certain classes of risk measures ρ, the algorithm produces a consistent estimate, i.e. if N and M are chosen *large enough*, $\rho(\hat{C}_\tau^{(M,N)})$ presents a viable approximation. In the next part, we make more precise what *large enough* means and, particularly, how large N needs to be chosen relative to M.

3.2 Joint Convergence and Convergence Rate

The LSM algorithm approximates the capital level – which is given by the conditional expectation of the aggregated future cash flows $V_\tau = \sum_{j=1}^{T} x_j(Y_j^{(i)})$ – by its linear projection on the subspace spanned by the basis functions $e^{(M)}(Y_\tau) = (e_1(Y_\tau), \ldots, e_M(Y_\tau))'$:

$$\mathbb{E}^{\tilde{\mathbb{P}}}\left[V_\tau | Y_\tau\right] \approx e^{(M)}(Y_\tau)'\, \hat{\alpha}^{(N)}.$$

Thus, the approximation takes the form of a *series estimator* for the conditional expectation. General conditions for the *joint* convergence of such estimators are provided in Newey (1997). Convergence of the risk measure then follows as in the previous subsection. We immediately obtain:[3]

Proposition 3.2 (Newey (1997))**.** *Assume* $Var(V_\tau|Y_\tau)$ *is bounded and that for every* M*, there is a non-singular constant matrix* B *such that for* $\tilde{e}^{(M)} = B\, e^{(M)}$ *we have:*

- *The smallest eigenvalue of* $\mathbb{E}^{\mathbb{P}}\left[\tilde{e}^{(M)}(Y_\tau)\,\tilde{e}^{(M)}(Y_\tau)'\right]$ *is bounded away from zero uniformly in* M*; and*
- *there is a sequence of constants* $\xi_0(M)$ *satisfying* $\sup_{y\in\mathcal{Y}} \|\tilde{e}^{(M)}(y)\| \leq \xi_0(M)$ *and* $M = M(N)$ *such that* $\xi_0(M)^2\, M/N \to 0$ *as* $N \to \infty$*, where* $\mathcal{Y}$ *is the support of* Y_τ*.*

Moreover, assume there exist $\psi > 0$ *and* $\alpha_M \in \mathbb{R}^M$ *such that* $\sup_{y\in\mathcal{Y}} |C_\tau(y) - e^{(M)}(y)'\,\alpha_M| = O(M^{-\psi})$ *as* $M \to \infty$*.*

Then:

$$\mathbb{E}^{\tilde{\mathbb{P}}}\left[\left(C_\tau - \hat{C}_\tau^{(M,N)}\right)^2\right] = O(M/N + M^{-2\,\psi}),$$

i.e. we have joint convergence in $L^2(\mathbb{R}^d, \mathcal{B}, \mathbb{P}_{Y_\tau})$*.*

In this result, we clearly see the influence of the two approximations: The functional approximation is reflected in the second part of the expression for the convergence rate. Here, it is worth noting that the speed ψ will depend on the choice of the basis functions, emphasizing the importance of this aspect. The first part of the expression corresponds to the regression approximation, and in line with the second part of Proposition 3.1 it goes to zero linearly in N.

The result provides general conditions that can be checked for any selection of basis functions, although ascertaining them for each underlying stochastic model may be cumbersome. Newey also provides explicit conditions for the practically relevant case of power series. In our notation, they read as follows:

Proposition 3.3 (Newey (1997))**.** *Assume* $Var(V_\tau|Y_\tau)$ *is bounded and that the basis functions* $e^{(M)}(Y_\tau)$ *consist of orthonormal polynomials, that* $\mathcal{Y}$ *is a Cartesian product of compact connected intervals, and that a sub-vector of* Y_τ *has a density that is bounded away from zero. Moreover, assume that* $C_\tau(y)$ *is continuously differentiable of order* s*.*

Then, if $M^3/N \to 0$*, we have:*

$$\mathbb{E}^{\tilde{\mathbb{P}}}\left[\left(C_\tau - \hat{C}_\tau^{(M,N)}\right)^2\right] = O(M/N + M^{-2s/d}),$$

i.e. we have joint convergence in $L^2(\mathbb{R}^d, \mathcal{B}, \mathbb{P}_{Y_\tau})$*.*

[3] Newey (1997) also provides conditions for uniform convergence and for asymptotic normality of series estimators. We refer to his paper for details.

Hence, for orthonormal polynomials, the smoothness of the conditional expectation is important – which is not surprising given Jackson's inequality. First-order differentiability is required ($s \geq 1$), and if $s = 1$, the convergence of the functional approximation will only be of order $M^{-2/d}$, where d is the dimension of the underlying model. Clearly, a more customized choice of the basis functions may improve on this rate.

We note that although M/N enters the convergence rate, the general conditions require $\xi_0(M)^2\, M/N \to 0$ in general and $M^3/N \to 0$ for orthonormal polynomials, effectively to control for the influence of estimation errors in the empirical covariance matrix of the regressors. Moreover, for common financial models the assumption of a bounded conditional variance or bounded support of the stochastic variables are not satisfied. Benedetti (2017) shows that if the distribution of the state process is known, convergence can still be ensured at a rate of $M^2 \log\{M\}/N \to 0$ under more modest – and in the financial context more appropriate – conditions. We refers to his paper for details.

Regarding the properties of the estimator beyond convergence, much rides on the first (functional) approximation that we discuss in more detail in the following Section 4. With regards to the second approximation, it is well-known that as the OLS estimate, $\widehat{C}_\tau^{(M,N)}$ is unbiased – though not necessarily efficient – for $\widehat{C}_\tau^{(M)}$ under mild conditions (see e.g. Sec. 6 in Amemiya (1985)). However, this clearly does not imply that $\rho(\widehat{C}_\tau^{(M,N)})$ is unbiased for $\rho(\widehat{C}_\tau^{(M)})$. Proceeding similarly to Gordy and Juneja (2010) for the nested simulations estimator, in the next subsection we analyze this relationship in more detail for VaR.

3.3 LSM Estimate for Value-at-Risk

VaR is an important special case, since it is the risk measure applied in regulatory frameworks, particularly Solvency II. VaR does not fall in the class of convex risk measures so that Corollary 3.1 does not apply. However, convergence immediately follows from Propositions 3.1-3.3:

Corollary 3.2. *We have:*

$$F_{\widehat{C}_\tau^{(M,N)}}(l) = \mathbb{P}(\widehat{C}_\tau^{(M,N)} \leq l) \to \mathbb{P}(C_\tau \leq l) = F_{C_\tau}(l),\ N \to \infty,\ M \to \infty,\ l \in \mathbb{R},$$

and:

$$F^{-1}_{\widehat{C}_\tau^{(M,N)}}(\alpha) \to F^{-1}_{C_\tau}(\alpha),\ N \to \infty,\ M \to \infty,$$

for all continuity points $\alpha \in (0,1)$ of $F^{-1}_{C_\tau}$. Moreover, under the conditions of Propositions 3.2 and 3.3, we have joint convergence.

Gordy and Juneja (2010) show that the nested simulations estimator for VaR carries a positive bias in the order of the number of simulations in the inner step. They derive their results by considering the joint density of the exact distribution of the capital at time τ and the error when relying on a finite number of inner simulations scaled by the square-root of the number of inner simulations. The following proposition establishes that their results carry over to our setting in view of the second approximation:

Proposition 3.4 (Gordy and Juneja (2010))**.** *Let $g_N(\cdot,\cdot)$ denote the joint probability density function of $(-\hat{C}_\tau^{(M)}, Z^{(N)})$, and assume that it satisfies the regularity conditions from Gordy and Juneja (2010) collected in the Appendix. Then:*

$$\mathbb{E}\left[\widehat{VaR}_\alpha\left[-\widehat{C}_\tau^{(M,N)}\right]\right] = VaR_\alpha\left[-\widehat{C}_\tau^{(M)}\right] + \frac{\theta_\alpha}{N\bar{f}\left(VaR_\alpha\left[-\widehat{C}_\tau^{(M)}\right]\right)} + o_N(N^{-1}),$$

where $\widehat{VaR}_\alpha\left[-\widehat{C}_\tau^{(M,N)}\right]$ denotes the $\lceil (1-\alpha)N \rceil$ order statistic of $\widehat{C}_\tau^{(M,N)}(Y_\tau^{(i)})$, $1 \le i \le N$ (the sample quantile), $\theta_\alpha = -\frac{1}{2}\frac{d}{d\mu}\left[\bar{f}(\mu)\mathbb{E}\left[\sigma^2_{Z^{(N)}}| - \widehat{C}_\tau^{(M)} = \mu\right]\right]_{\mu=VaR_\alpha\left[-\widehat{C}_\tau^{(M)}\right]}$, $\sigma^2_{Z^{(N)}} = \mathbb{E}\left[\left(Z^{(N)}\right)^2|Y_\tau\right]$, and $\bar{f}$ is the marginal density of $-\widehat{C}_\tau^{(M)}$.

The key point of the proposition is that – similarly to the nested simulations estimator – the LSM estimator for VaR is biased. In particular, for large losses or a large value of α, the derivative of the density in the tail is negative resulting in a positive bias. That is, ceteris paribus, on average the LSM estimator will err on the "conservative" side (see also Bauer et al. (2012b)). However, note that this statement of course ignores the variance due to estimating the risk measure from the finite sample, which trumps the inaccuracy due to bias – and unlike the nested simulations setting, here the two sources are governed by the same parameter N. Indeed, as is clear from Proposition 3.1, the convergence of the variance is of order N and thus dominates the mean squared error for relatively large values of N (the bias will enter as $O(N^{-2})$). Moreover, of course the result only pertains to the regression approximation but not the approximation of the capital variable via the linear combination of basis functions, which is at the core of the proposed algorithm.

4 Choice of Basis Functions

As demonstrated in Section 3.1, any set of independent functions will lead the LSM algorithm to converge. In fact, for the LSM method for pricing non-European derivatives, frequent choices of basis functions include Hermite polynomials, Legendre polynomials, Chebyshev polynomials, Fourier series, and even simple polynomials. While the choice is important for the pricing approximation (Glasserman, 2004, Sec. 8.6), several authors conclude based on numerical tests that the approach appears robust for typical problems when including a sufficiently large number of terms (see e.g. Moreno and Navas (2003) and also the original paper by Longstaff and Schwartz (2001)). A key difference between the LSM pricing method and the approach here, however, is that it is necessary to approximate the distribution over its entire domain rather than the expected value only. Furthermore, the state space for estimating a company's capital can be high-dimensional and considerably more complex than that of a derivative security. Therefore, the choice of basis functions is not only potentially more complex but also more crucial in the present context.

4.1 Optimal Basis Functions for a Model Framework

As illustrated in Section 2.1, we can identify capital – as a function of the state vector at the risk horizon Y_τ – for a cash flow *model* $\mathbf{x}$ within a certain *model framework* Y with the output

of the linear operator L applied to $\mathbf{x}$: $C_\tau(Y_\tau) = L\mathbf{x}(Y_\tau)$ (Eq. (3)). As discussed in Section 3.2, the LSM algorithm, in turn, approximates C_τ by its linear projection on the subspace spanned by the basis functions $e^{(M)}(Y_\tau)$, $P\,C_\tau(Y_\tau)$, where P is the projection operator.

For simplicity, in what follows, we assume that the basis functions are orthonormal in $L^2(\mathbb{R}, \mathcal{B}, \mathbb{P}_{Y_\tau})$. Then we can represent P as:

$$P\cdot = \sum_{k=1}^{M} \langle \cdot, e_k(Y_\tau) \rangle_{L^2(\mathbb{P}_{Y_\tau})}\, e_k.$$

Therefore, the LSM approximation can be represented via the *finite rank* operator $L_F = P\,L$, where we have:

$$\begin{aligned} L_F\mathbf{x} &= P\,L\,\mathbf{x} = \sum_{k=1}^{M} \langle L\mathbf{x}, e_k(Y_\tau) \rangle_{L^2(\mathbb{P}_{Y_\tau})}\, e_k \\ &= \sum_{k=1}^{M} \mathbb{E}^{\mathbb{P}}\left[e_k(Y_\tau) \sum_{j=\tau}^{T} \mathbb{E}^{\tilde{\mathbb{P}}}\left[x_j(Y_j) | Y_\tau \right] \right] e_k = \sum_{k=1}^{M} \mathbb{E}^{\mathbb{P}}\left[e_k(Y_\tau) \underbrace{\sum_{j=\tau}^{T} x_j(Y_j)}_{=V_\tau} \right] e_k \\ &= \sum_{k=1}^{M} \underbrace{\mathbb{E}^{\tilde{\mathbb{P}}}\left[e_k(Y_\tau)\, V_\tau \right]}_{\alpha_k} e_k, \end{aligned} \tag{7}$$

where the fourth equality follows by the tower property of conditional expectations.

It is important to note that under this representation, ignoring the uncertainty arising from the regression estimate, the operator L_F gives the LSM approximation for *each* model $\mathbf{x}$ within the *model framework*. That is, the choice of the basis function *precedes* fixing a particular cash flow model (payoff). Thus, we can define *optimal basis functions* as a system that minimizes the distance between L and L_F, so that the approximation is optimal with regards to all possible cash flow models within the framework:

Definition 4.1. *We call the set of basis functions* $\{e_1^*, e_2^*, ..., e_M^*\}$ *optimal in* $L^2(\mathbb{R}^d, \mathcal{B}, \mathbb{P}_{Y_\tau})$ *if:*

$$\{e_1^*, e_2^*, ..., e_M^*\} = \operatorname{arginf}_{\{e_1, e_2, ..., e_M\}} \|L - L_F\| = \operatorname{arginf}_{\{e_1, e_2, ..., e_M\}} \sup_{\|\mathbf{x}\|=1} \|L\mathbf{x} - L_F\mathbf{x}\|.$$

This notion of *optimality* has various advantages in the context of calculating risk capital. Unlike pricing a specific derivative security with a well-determined payoff, capital may need to be calculated for subportfolios or only certain lines of business for the purpose of capital allocation (Bauer and Zanjani, 2016). Moreover, a company's portfolio will change from one calculation date to the next, so that the relevant cash flow model is in flux. The underlying model framework, on the other hand, is usually common to all subportfolios since the purpose of a capital framework is exactly the enterprise-wide determination of diversification opportunities and systematic risk factors. Also, it is typically not frequently revised. Hence, it is expedient here to connect the optimality of basis functions to the framework rather than a particular model (payoff).

4.2 Optimal Basis Functions for a Compact Valuation Operator

In order to derive optimal basis functions, it is sufficient to determine the finite-rank operator L_F that presents the best approximation to the infinite-dimensional operator L. If L is a compact operator, this approximation is immediately given by the *singular value decomposition* (SVD) of L (for convenience, details on the SVD of a compact operator are collected in the Appendix). More precisely, we can then represent $L : \mathcal{H} \to L^2(\mathbb{R}^d, \mathcal{B}, \mathbb{P}_{Y_\tau})$ as:

$$L\,\mathbf{x} = \sum_{k=1}^{\infty} \omega_k \,\langle \mathbf{x}, s_k \rangle\, \varphi_k, \tag{8}$$

where $\{\omega_k\}$ with $\omega_1 \geq \omega_2 \geq \ldots$ are the singular values of L, $\{s_k\}$ are the right singular functions of L, and $\{\varphi_k\}$ are the left singular functions of L – which are exactly the eigenfunctions of $L\,L^*$. The following proposition demonstrates that the optimal basis functions are given by the left singular functions of L.

Proposition 4.1. *Assume the operator L is compact. Then for each M, the left singular functions of L $\{\varphi_1, \varphi_2, \ldots, \varphi_M\} \in L^2(\mathbb{R}^d, \mathcal{B}, \mathbb{P}_{Y_\tau})$ are optimal basis functions in the sense of Definition 4.1. For a fixed cash flow model, we obtain $\alpha_k = \omega_k \langle \mathbf{x}, s_k \rangle$.*

Our finding that the left singular functions provide an optimal approximation is related to familiar results in finite dimensions. In particular, our proof is similar to the Eckart-Young-Mirsky Theorem on low-rank approximations of an arbitrary matrix. A sufficient condition for the compactness of the operator L is provided in Lemma 2.3.

To appraise the impact of the two approximations simultaneously, we can analyze the joint convergence properties in M and N for the case of optimal basis functions. Here, in general, we have to check the conditions from Newey's convergence result (Prop. 3.2). We observe that the convergence rate associated with the first (functional) approximation depends on the parameter ψ, which in the present context derives from the speed of convergence of the singular value decomposition:

$$\begin{aligned} O(M^{-\psi}) = \inf_{\alpha_M} \sup_{y \in \mathcal{Y}} |C_\tau(y) - e^{(M)}(y)'\,\alpha_M| &\leq \sup_{y \in \mathcal{Y}} |\,L\,\mathbf{x}\,(y) - L_F\,\mathbf{x}\,(y)| \\ &= \sup_{y \in \mathcal{Y}} \left| \sum_{k=M+1}^{\infty} \omega_k \,\langle \mathbf{x}, s_k \rangle\, \varphi_k(y) \right|. \end{aligned} \tag{9}$$

In particular, we are able to provide an explicit result in the case of bounded singular functions.

Proposition 4.2. *Assume $Var(V_\tau|Y_\tau)$ is bounded and that the singular functions, $\{\varphi_k\}_{k=1}^{\infty}$, are uniformly bounded on the support of Y_τ. Then, if $M^2/N \to 0$, we have:*

$$\mathbb{E}^{\tilde{\mathbb{P}}}\left[\left(C_\tau - \hat{C}_\tau^{(M,N)} \right)^2 \right] = O(M/N + \omega_M^2),$$

i.e. we have joint convergence in $L^2(\mathbb{R}^d, \mathcal{B}, \mathbb{P}_{Y_\tau})$.

Comparing this convergence rate for singular functions to the general case from Proposition 3.2 and the orthonormal polynomial case from Proposition 3.3, we notice that the second term associated with the first (functional) approximation now is directly linked to the decay of the singular values. For integral operators, this rate depends on the smoothness of the kernel $k(x, y)$ (see Birman and Solomyak (1977) for a survey on the convergence of singular values of integral operators). In any case, Equation (9) that directly enters Newey's convergence result illustrates the intuition behind the optimality criterion: To choose a basis function that minimizes the distance between the operators for all $\mathbf{x}$, although in the Definition we consider the L^2-norm rather than the supremum.

The derivation of the SVD of the valuation operator of course depends on the specific model framework. In some cases, it is possible to carry out the calculations and derive analytical expressions for the singular values. In the next subsection, we determine the SVD – and, thus, optimal basis functions – in the practically highly relevant case of Gaussian transition densities. Here, the optimal basis functions correspond to Hermite polynomials of suitably transformed state variables and the singular values decay exponentially for $d = 1$ (Proposition 4.3), demonstrating the merit of this choice.

4.3 Optimal Basis Functions for Gaussian Transition Densities

In what follows, we consider a single cash flow at time T only (generalizations follow analogously), and we assume that (Y_τ, Y_T) are jointly Gaussian distributed. We denote the $\tilde{\mathbb{P}}$-distribution of this random vector via:

$$\begin{pmatrix} Y_\tau \\ Y_T \end{pmatrix} \sim N\left[\begin{pmatrix} \mu_\tau \\ \mu_T \end{pmatrix}, \quad \begin{pmatrix} \Sigma_\tau & \Gamma \\ \Gamma' & \Sigma_T \end{pmatrix} \right], \tag{10}$$

where μ_τ, μ_T, Σ_τ, and Σ_T are the mean vectors and variance-covariance matrices of Y_τ and Y_T, respectively, and Γ is the corresponding (auto) covariance matrix – which we assume to be non-singular.

Denoting by $g(x; \mu, \Sigma)$ the normal probability density function at x with mean vector μ and covariance matrix Σ, the marginal densities of Y_τ and Y_T are $\pi_{Y_\tau}(x) = g(x; \mu_\tau, \Sigma_\tau)$ and $\pi_{Y_T}(y) = g(y; \mu_T, \Sigma_T)$, respectively. Mapping these assumption to the previous notation yields $\mathbf{x} = x_T$, $L : \mathcal{H} = L^2(\mathbb{R}^d, \mathcal{B}, \pi_{Y_T}) \to L^2(\mathbb{R}^d, \mathcal{B}, \pi_{Y_\tau})$, and:

$$C_\tau(Y_\tau) = L\mathbf{x}(Y_\tau) = \int_{\mathbb{R}^d} x_T(y)\, \pi_{Y_T|Y_\tau}(y|Y_\tau)\, dy,$$

where $\pi_{Y_T|Y_\tau}(y|x)$ denotes the transition density. In order to obtain optimal basis functions, the objective is to derive the SVD of L.

Lemma 4.1. *We have for the conditional distributions:*

$$Y_T|Y_\tau = x \sim N\left(\mu_{T|\tau}(x), \Sigma_{T|\tau}\right) \text{ and } Y_\tau|Y_T = y \sim N\left(\mu_{\tau|T}(y), \Sigma_{\tau|T}\right)$$

with transition density and reverse transition density:

$$\pi_{Y_T|Y_\tau}(y|x) = g(y; \mu_{T|\tau}(x), \Sigma_{T|\tau}) \text{ and } \pi_{Y_\tau|Y_T}(x|y) = g(x; \mu_{\tau|T}(y), \Sigma_{\tau|T}),$$

respectively, where $\mu_{T|\tau}(x) = \mu_T + \Gamma'\Sigma_\tau^{-1}(x - \mu_\tau)$, $\Sigma_{T|\tau} = \Sigma_T - \Gamma'\Sigma_\tau^{-1}\Gamma$, $\mu_{\tau|T}(y) = \mu_\tau + \Gamma\Sigma_T^{-1}(y - \mu_T)$, *and* $\Sigma_{\tau|T} = \Sigma_\tau - \Gamma\Sigma_T^{-1}\Gamma'$. *Moreover, L is compact in this setting.*

Per Proposition 4.1, the optimal basis functions are given by the left singular functions, which are in turn the eigenfunctions of $L\,L^*$. We obtain:

Lemma 4.2. *The operator LL^* and L^*L are integral operators:*

$$LL^*f(\cdot) = \int_{\mathbb{R}^d} K_A(\cdot, y)\, f(y)\, dy \text{ and } L^*Lf(\cdot) = \int_{\mathbb{R}^d} K_B(\cdot, x)\, f(x)\, dx,$$

where the kernels are given by Gaussian densities:

$$K_A(x, y) = g(y; \mu_A(x), \Sigma_A) \text{ and } K_B(y, x) = g(x; \mu_B(y), \Sigma_B)$$

with

- $\mu_A(x) = \mu_\tau + A(x - \mu_\tau)$, $A = \Gamma\Sigma_T^{-1}\Gamma'\Sigma_\tau^{-1}$, *and* $\Sigma_A = \Sigma_\tau - A\Sigma_\tau A'$;
- $\mu_B(y) = \mu_T + B(y - \mu_T)$, $B = \Gamma'\Sigma_\tau^{-1}\Gamma\Sigma_T^{-1}$, *and* $\Sigma_B = \Sigma_T - B\Sigma_T B'$.

We denote by $\mathbb{E}_{K_A}[\cdot|x]$ and $\mathbb{E}_{K_B}[\cdot|y]$ the expectation operators under the Gaussian densities $K_A(x, \cdot)$ and $K_B(y, \cdot)$, respectively.

The problem of finding the singular values and the left singular functions therefore amounts to solving the eigen-equations:

$$\mathbb{E}_{K_A}\left[f(Y)|x\right] = \omega^2\, f(x).$$

We exploit analogies to the eigenvalue problem of the Markov operator of a first-order multivariate normal autoregressive (MAR(1)) process studied in Khare and Zhou (2009) to obtain the following:

Lemma 4.3. *Denote by $P\Lambda P'$ the eigenvalue decomposition of:*

$$\Sigma_\tau^{-1/2}\, A\, \Sigma_\tau^{1/2} = \Sigma_\tau^{-1/2}\, \Gamma\Sigma_T^{-1}\Gamma'\Sigma_\tau^{-1/2},$$

where $PP' = I$ and Λ is the diagonal matrix whose entries are the eigenvalues $\lambda_1 \geq \lambda_2 \geq \cdots \geq \lambda_d$ of A. For $y \in \mathbb{R}^d$, define the transformation:

$$z^P(y) = P'\Sigma_\tau^{-1/2}(y - \mu_\tau). \tag{11}$$

Then for $Y \sim K_A(x, \cdot)$, we have:

$$\mathbb{E}_{K_A}\left[z^P(Y)|x\right] = \Lambda\, z^P(x).$$

Moreover, $Var_{K_A}\left[z^P(Y)|x\right] = I - \Lambda^2$, $\mathbb{E}_{\pi_{Y_\tau}}\left[z^P(Y_\tau)\right] = 0$, and $Var_{\pi_{Y_\tau}}\left[z^P(Y_\tau)\right] = I$.

Similarly, denote the diagonalization $\Sigma_T^{-1/2}B\Sigma_T^{1/2} = Q\Lambda Q'$, where $Q'Q = I$ and define the transformation:

$$z^Q(x) = Q'\Sigma_T^{-1/2}(x - \mu_T). \tag{12}$$

Then for $X \sim K_B(y, \cdot)$, we have:

$$\mathbb{E}_{K_B}\left[z^Q(X)|y\right] = \Lambda\, z^Q(y),$$

$Var_{K_B}\left[z^Q(X)|y\right] = I - \Lambda^2$, $\mathbb{E}_{\pi_{Y_T}}\left[z^Q(Y_T)\right] = 0$, *and* $Var_{\pi_{Y_T}}\left[z^Q(Y_T)\right] = I$.

Therefore, for a random vector $Y|x$ in $\mathbb{R}^d$ that is distributed according to $K_A(x,\cdot)$, the components $z_i^P(Y)$ of $z^P(Y)$ are independently distributed with $z_i^P(Y) \sim N(\lambda_i\, z_i^P(x), 1-\lambda_i^2)$, where $z_i^P(x)$ is the i-th component of $z^P(x)$. Since eigenfunctions of standard Gaussian distributed random variables are given by Hermite polynomials, the SVD follows immediately from Lemma 4.3:

Proposition 4.3. *Denote the Hermite polynomial of degree j by $h_j(x)$ (Kollo and Rosen, 2006):*

$$h_0(x) = 1,\ h_1(x) = x,\ h_j(x) = \frac{1}{\sqrt{j}}\left(x\, h_{j-1}(x) - \sqrt{j-1}h_{j-2}(x)\right), \quad j = 2, 3, ...$$

The singular values of L in the current (Gaussian) setting are given by:

$$\omega_m = \Pi_{i=1}^d \lambda_i^{k_i/2}, \quad m = (k_1, ..., k_d) \in \mathbb{N}_0^d, \tag{13}$$

where $\mathbb{N}_0^d$ is the set of d-dimensional non-negative integers, and the corresponding right and left singular functions are:

$$s_m(x) = \Pi_{i=1}^d h_{k_i}(z_i^Q(x)) \text{ and } \varphi_m(y) = \Pi_{i=1}^d h_{k_i}(z_i^P(y)),$$

respectively.

Combining the insights from Proposition 4.1 and Proposition 4.3, we immediately obtain:

Corollary 4.1. *Let $(m_k)_{k\in\mathbb{N}}$ be a reordering of $\{m\} = \{(k_1, ..., k_d) \in \mathbb{N}_0^d\}$ such that:*

$$\omega_{m_1} \geq \omega_{m_2} \geq \omega_{m_3} \geq \dots$$

Then, in the current setting, optimal choices for the basis functions for the LSM algorithm in the sense of Definition 4.1 are given by:

$$\varphi_k = \varphi_{m_k},\ k = 1, 2, 3, \dots$$

In the univariate case ($d = 1$), $A = \lambda_1$ is the square of the correlation coefficient between Y_τ and Y_T – so that the singular values are simply powers of this correlation, decaying exponentially. Thus, the SVD takes the form (Abbe and Zheng, 2012):

$$L\,\mathbf{x}(Y_\tau) = \sum_{k=1}^{\infty} \left(\mathrm{Corr}(Y_\tau, Y_T)\right)^{k-1} \left\langle x_T, h_{k-1}\left(\frac{Y_T - \mu_T}{\Sigma_T}\right)\right\rangle_{\pi_{Y_T}} h_{k-1}\left(\frac{Y_\tau - \mu_\tau}{\Sigma_\tau}\right).$$

In particular, optimal basis functions are given by Hermite polynomials of the normalized Markov state – although other choices of polynomial bases will generate the same span so that the results will coincide.

In the general multivariate case, it is clear from Proposition 4.3 that the singular values of L are directly related to eigenvalues of the matrix A (or, equivalently, B), and there are $\binom{d-1+l}{d-1}$ vectors of indices m such that $\sum_i k_i = l$ in Equation (13) (stars and bars problem). The order of these singular values will determine the order of the singular functions in the

SVD (8). In particular, after $\varphi_1(x) = 1$ with coefficient equaling $\langle x_T, 1\rangle = \mathbb{E}[x_T]$, the first nontrivial basis function is given by the singular function associated with the largest singular value – which according to (11) is a component of the linearly transformed normalized state vector. The subsequent basis functions depend on the relative magnitudes of the different singular values. For instance, while for $1 > \lambda_1 > \lambda_2$ clearly $\sqrt{\lambda_1} > \sqrt{\lambda_1}^2 = \lambda_1$ and similarly for λ_2, it is not clear whether $\lambda_1 > \sqrt{\lambda_2}$ or vice versa – and this order will determine which combination of basis functions is optimal.

Thus, in the multi-dimensional case – and particularly in high-dimensional settings that are relevant for practical applications – is where the analysis here provides immediate guidance. Even if a user chooses the same function class (Hermite polynomials) or function classes with the same span (e.g., other polynomial families), it is unlikely that a naïve choice will pick the suitable combinations – and this choice becomes less trivial and more material as the number of dimensions increases.

From Proposition 3.1, we obtain sequential convergence. Joint convergence for (a class of) models $\mathbf{x}$ can be established by following Newey's approach from Propositions 3.2/3.3, or by relying on the results from Benedetti (2017) in case the parameters are known. While the Hermite polynomials do not satisfy the uniformly boundedness assumptions from Proposition 4.2, from Proposition 3.2 and the discussion following Proposition 4.2, it is clear that the convergence rate of the functional approximation is linked to the decay of the singular values ($O(\omega_M^2)$ in Prop. 4.2). In the current setting we have (Prop. 4.3):

$$\omega_M^2 = \omega_{m_M}^2 = \prod_{i=1}^{d} \lambda_i^{k_i} \leq \prod_{i=1}^{d} \max_{1\leq i\leq d}\{\lambda_i\}^{k_i} = \max_{1\leq i\leq d}\{\lambda_i\}^{\sum_i k_i},$$

where $\max_{1\leq i\leq d}\{\lambda_i\} < 1$ and there are $\binom{d-1+l}{d-1}$ vectors m such that $\sum_i k_i = l$. Thus, as in Proposition 3.3, the convergence is slowing down as the dimension d of the state process increases, although the relationship here is exponential rather than polynomial.

In models with non-Gaussian transitions, while an analytical derivation may not be possible, we can rely on numerical methods to determine approximations of the optimal basis functions. For instance, Huang (2012) explains how to solve the associated integral equation by discretization methods, which allows to determine the singular functions numerically, and Serdyukov et al. (2014) apply the truncated SVD to solve inverse problems numerically. Alternatively, one can approximate an arbitrary distribution by a Gaussian distributions using the first two (possible sample) moments to obtain approximately optimal basis functions. Using a Gaussian approximation is common in statistical learning applications, for instance in Discriminant Analysis (Hastie et al., 2009).

5 Application

To illustrate the LSM algorithm and its properties, we consider an example from life insurance: a Guaranteed Minimum Income Benefit (GMIB) within a Variable Annuity contract. As indicated in the Introduction, the LSM algorithm is particularly relevant in insurance, especially in light of the new Solvency II regulation that came into effect in 2016. Here, the so-called *Solvency Capital Requirement* takes the form of a 99.5% VaR at the risk horizon $\tau = 1$.

Within a Variable Annuity (VA) plus GMIB contract, at maturity T the policyholder has the right to choose between a lump sum payment amounting to the current account value or a guaranteed annuity payment b determined by a guaranteed rate applied to a guaranteed amount. GMIBs are popular riders for VA contracts: Between 2011 and 2013, roughly 15% of the more than $150 billion worth of Variable Annuities sold in the US contained a GMIB.[4] Importantly, GMIBs are subject to a variety of risk factors, including fund (investment) risk, mortality risk, and – as long term contracts – interest rate risk. Consequently, we consider its risk and valuation in a multivariate Markov setting for these three risk factors.

5.1 Model and Payoff of the GMIB

We consider a large portfolio of GMIBs with policyholder age x, policy maturity T, and a fixed guaranteed amount – so that the guaranteed annuity payment b is fixed at time zero. The payoff of the VA plus GMIB at T in case of survival is given by:

$$\max\left\{S_T,\ b\, a_{x+T}(T)\right\}, \tag{14}$$

where S_T is the underlying account value which evolves according to a reference asset net various fees (which we ignore for simplicity) and $a_{x+T}(T)$ denotes the time T value of an immediate annuity on an $(x+T)$-year old policyholder of $1 annually.

We consider a three-dimensional state process Y_t governing financial and biometric risks:

$$Y_t = (q_t,\, r_t,\, \mu_{x+t})',$$

where q_t denotes the log-price of the risky asset at time t, r_t is the short rate, and μ_{x+t} is the force of mortality of an $(x+t)$-aged person at time t. We assume Y_t satisfies the following stochastic differential equations under $\mathbb{P}$:

$$dq_t = \left(m - \frac{1}{2}\sigma_S^2\right) dt + \sigma_S\, dW_t^S, \tag{15}$$

$$dr_t = \alpha(\gamma - r_t)\, dt + \sigma_r\, dW_t^r, \tag{16}$$

$$d\mu_{x+t} = \kappa\mu_{x+t}\, dt + \psi\, dW_t^\mu, \tag{17}$$

where m is the instantaneous rate of return of the risky asset and σ_S is the asset volatility; α, γ, and σ_r are the speed of mean reversion, the mean reversion level, and the interest rate volatility in the Vasicek (1977) interest rate model, respectively; κ is an instantaneous rate of increment of mortality (Gompertz exponent) and ψ is the volatility of mortality; and W_t^S, W_t^r, and W_t^μ are standard Brownian motions under $\mathbb{P}$ with $dW_t^S\, dW_t^r = \rho_{12}\, dt$, $dW_t^S\, dW_t^\mu = \rho_{13}\, dt$, and $dW_t^r\, dW_t^\mu = \rho_{23}\, dt$. Note that the solutions to the above stochastic differential equations ensure that (Y_t, Y_T) is Gaussian, so that we can derive the optimal basis function using the approach in Section 4.3.

The dynamics of Y_t under the risk-neutral measure $\mathbb{Q}$ are given by:

$$dq_t = \left(r_t - \frac{1}{2}\sigma_S^2\right) dt + \sigma_S\, d\tilde{W}_t^S,$$

$$dr_t = \alpha(\bar{\gamma} - r_t)\, dt + \sigma_r\, d\tilde{W}_t^r,$$

$$d\mu_{x+t} = \kappa\mu_{x+t}\, dt + \psi\, d\tilde{W}_t^\mu,$$

[4]Source: Fact Sheets by the Life Insurance and Market Research Association (LIMRA).

where $\tilde{W}_t^S$, $\tilde{W}_t^r$, and $\tilde{W}_t^\mu$ are standard Brownian motions under $\mathbb{Q}$ with the same correlation coefficients. Here, for simplicity, we assume that there is no risk premium for mortality risk and we assume a constant risk premium λ for interest rate risk, resulting in $\bar{\gamma} = \gamma - \lambda\,\sigma_r/\alpha$. Hence, the time-$t$ value of the VA plus GMIB contract is:

$$V(t) = \mathbb{E}^{\mathbb{Q}}\left[e^{-\int_t^T r_s+\mu_{x+s}\,ds}\max\left\{e^{q_T},\ b\,a_{x+T}(T)\right\}|Y_t\right]. \tag{18}$$

Since it is not possible to obtain an analytical expression for the GMIB, particularly when considering additional features such as step ups or ratchets, it is necessary to rely on numerical methods for valuation and estimating risk capital. To directly apply our LSM framework, we adjust the presentation by changing the numéraire to a pure endowment (survival benefit) with maturity T and maturity value one. The price of the VA plus GMIB at time t is then:

$$V(t) = {}_{T-t}E_{x+t}\,\mathbb{E}^{\mathbb{Q}_E}\left[\max\left\{e^{q_T},\ b\,a_{x+T}(T)\right\}|Y_t\right], \tag{19}$$

where $\tau \le t \le T$, ${}_{T-t}E_{x+t}$ is the price of the pure endowment contract at time t, and $\mathbb{Q}_E$ is the risk-neutral measure using the pure endowment contract as the numéraire.

Under our assumption, we obtain:

$${}_{T-t}E_{x+t}(Y_t) \;=\; \mathbb{E}^{\mathbb{Q}}\left[e^{-\int_t^T r_s+\mu_{x+s}\,ds}|Y_t\right] = A(t,T)\exp\left[-B_r(t,T)r_t - B_\mu(t,T)\mu_{x+t}\right]$$

since (r_t) and (μ_t) are affine with:

$$\begin{aligned}
B_r(t,T) &= \frac{1-e^{-\alpha(T-t)}}{\alpha},\ B_\mu(t,T) = \frac{e^{\kappa(T-t)}-1}{\kappa},\\
\text{and } A(t,T) &= \exp\left\{\bar{\gamma}\left(B_r(t,T)-T+t\right) + \frac{1}{2}\left\{\frac{\sigma_r^2}{\alpha^2}\left(T-t-2B_r(t,T)+\frac{1-e^{-2\alpha(T-t)}}{2\alpha}\right)\right.\right.\\
&\quad + \frac{\psi^2}{\kappa^2}\left(T-t-2B_\mu(t,T)+\frac{e^{2\kappa(T-t)}-1}{2\kappa}\right)\\
&\quad \left.\left. + \frac{2\rho_{23}\sigma_r\psi}{\alpha\kappa}\left(B_\mu(t,T)-T+t+B_r(t,T)-\frac{1-e^{-(\alpha-\kappa)(T-t)}}{\alpha-\kappa}\right)\right\}\right\}.
\end{aligned}$$

Thus, applying Itô's formula, the dynamics of the pure endowment price are:

$$d_{T-t}E_{x+t} = {}_{T-t}E_{x+t}\left[(r_t+\mu_{x+t})dt - \sigma_r B_r(t,T)d\tilde{W}_t^r - \psi B_\mu(t,T)d\tilde{W}_t^\mu\right],$$

and from Brigo and Mercurio (2006), the new dynamics of Y_t under $\mathbb{Q}_E$ for $\tau \le t \le T$ become:

$$dq_t = \left(r_t - \frac{1}{2}\sigma_S^2 - \rho_{12}\sigma_S\sigma_r B_r(t,T) - \rho_{13}\sigma_S\psi B_\mu(t,T)\right)dt + \sigma_S dZ_t^S, \tag{20}$$

$$dr_t = \left(\alpha(\bar{\gamma}-r_t) - \sigma_r^2 B_r(t,T) - \rho_{23}\sigma_r\psi B_\mu(t,T)\right)dt + \sigma_r dZ_t^r, \tag{21}$$

$$d\mu_{x+t} = \left(\kappa\mu_{x+t} - \rho_{23}\sigma_r\psi B_r(t,T) - \psi^2 B_\mu(t,T)\right)dt + \psi\,dZ_t^\mu, \tag{22}$$

where Z_t^S, Z_t^r, and Z_t^μ are standard Brownian motions under $\mathbb{Q}_E$ with $dZ_t^S dZ_t^r = \rho_{12}\,dt$, $dZ_t^S dZ_t^\mu = \rho_{13}\,dt$, and $dZ_t^r dZ_t^\mu = \rho_{23}\,dt$.

For the calculation of the risk capital for the VA plus GMIB contract, we ignore unsystematic mortality risk arising from finite samples and stochastic investments, and we estimate the risk measure $\rho(V(\tau, Y_\tau))$ via the LSM algorithm. In particular, the cash flow functional in the current setting is $\mathbf{x} = x_T$ with:

$$x_T(Y_T) = -V(T) = -\max\{e^{q_T}, b\underbrace{\sum_{k=1}^{\infty} {}_kE_{x+T}(Y_T)}_{=a_{x+T}(T)}\}$$

and

$$C_\tau = L\,\mathbf{x}(Y_\tau) = {}_{T-\tau}E_{x+\tau}(Y_\tau)\,\mathbb{E}^{\mathbb{Q}_E}\left[x_T(Y_T)|Y_\tau\right].$$

To apply our results on optimal basis functions, we require the joint distribution of Y_τ and Y_T:

Lemma 5.1. *From (15)–(17) and (20)–(22), the joint (unconditional) distribution of Y_τ and Y_T under $\tilde{\mathbb{P}}$ is:*

$$\begin{pmatrix} Y_\tau \\ Y_T \end{pmatrix} \sim N\left[\begin{pmatrix} \mu_\tau \\ \mu_T \end{pmatrix}, \quad \begin{pmatrix} \Sigma_\tau & \Gamma \\ \Gamma' & \Sigma_T \end{pmatrix}\right],$$

where we refer to the proof in the Appendix for explicit expressions of μ_τ, μ_T, Σ_τ etc. in terms of the parameters.

Thus we can apply the results from Proposition 4.3 to derive optimal basis functions. More precisely, for any non negative integer vector $l = (l_1, l_2, l_3)$, $\omega_{|l|} = \lambda_1^{l_1}\lambda_2^{l_2}\lambda_3^{l_3}$ is a squared singular value of L, and the corresponding left singular functions is:

$$\varphi_l(x) = h_{l_1}(z_1^P(x))h_{l_2}(z_2^P(x))h_{l_3}(z_3^P(x)).$$

Thus, in order to find the set of optimal basis functions for the LSM algorithm consisting of M functions, we need to calculate $\omega_{|m|}$ for $m = (m_1, m_2, m_3)$ such that $|m| \leq M$, order them, and then determine the associated functions.

5.2 Numerical Results

We set the model parameters using representative values. The initial price of the risky asset is one hundred – so $q_0 = 4.605$ – and for the risky asset parameters we assume $m = 5\%$ (instantaneous rate of return) and $\sigma_S = 18\%$ (asset volatility). The initial interest rate is assumed to be $r_0 = 2.5\%$, $\alpha = 25\%$ (speed of mean reversion), $\gamma = 2\%$ (mean reversion level), $\sigma_r = 1\%$ (interest rate volatility), and $\lambda = 2\%$ (market price of risk). For the mortality rate, we set $x = 55$ (age of the policyholder), $\mu_{55} = 1\%$ (initial value of mortality), $\kappa = 7\%$ (instantaneous rate of increment), and $\psi = 0.12\%$ (mortality volatility). For correlations, we assume $\rho_{12} = -30\%$ (correlation between asset and interest rate), $\rho_{13} = 6\%$ (correlation between asset and mortality rate), and $\rho_{23} = -4\%$ (correlation between interest rate and mortality rate). For the insurance contract, we let the maturity $T = 15$ and we set:

$$b = S_0 \times {}^{(1+m_g)^T}\!/_{a^*_{x+T}} = S_0 \times {}^{(1+m_g)^T({}_TE_x(Y_0))}\!/_{\left(\sum_{k=1}^{\infty} {}_{T+k}E_x(Y_0)\right)},$$

where we assume a guaranteed rate of return $m_g = 2\%$ and a^*_{x+T} is the annuity value based on forward mortality rates (Bauer et al., 2012a). This implies a probability that $S_T > b\, a_{x+T}(T)$ of approximately 40%. Finally, we set the risk horizon $\tau = 1$ in line with the Solvency II regulation.

With the above parameters, the eigenvalues of A in Lemma 4.3 are $\lambda_1 = 0.14898$, $\lambda_2 = 0.06712$, and $\lambda_3 = 0.00035$. The first singular value of the valuation operator in Proposition 4.3 is one and its corresponding left singular function is $\varphi_1(x) = 1$. The second singular value is $\sqrt{\lambda_1}$ and the corresponding left singular function is $\varphi_2(x) = z_1^P(x)$. The next three singular values are given by $\sqrt{\lambda_2}$, λ_1, and $\sqrt{\lambda_1\lambda_2}$, and the corresponding left singular functions are $\varphi_3(x) = z_2^P(x)$, $\varphi_4(x) = \frac{1}{\sqrt{2}}\left(\left(z_1^P(x)\right)^2 - 1\right)$, and $\varphi_5(x) = z_1^P(x)z_2^P(x)$, respectively. In contrast, a naïve choice of five monomials may result in the sequence $(1, q_\tau, r_\tau, \mu_{x+\tau}, q_\tau^2)$ or another arbitrary arrangement.

Functional approximation.

We implement the LSM approximation to the capital variable and vary the number of basis functions. In Figure 1, we provide an empirical density based on $N = 3,000,000$ and approximate realizations calculated via the LSM algorithm for different numbers of basis functions M.[5] Here we rely on the optimal basis functions from above. As is evident from the figure, a small number of basis function does not produce satisfactory results. However, the approximation becomes closer to the "exact" density as M increases.

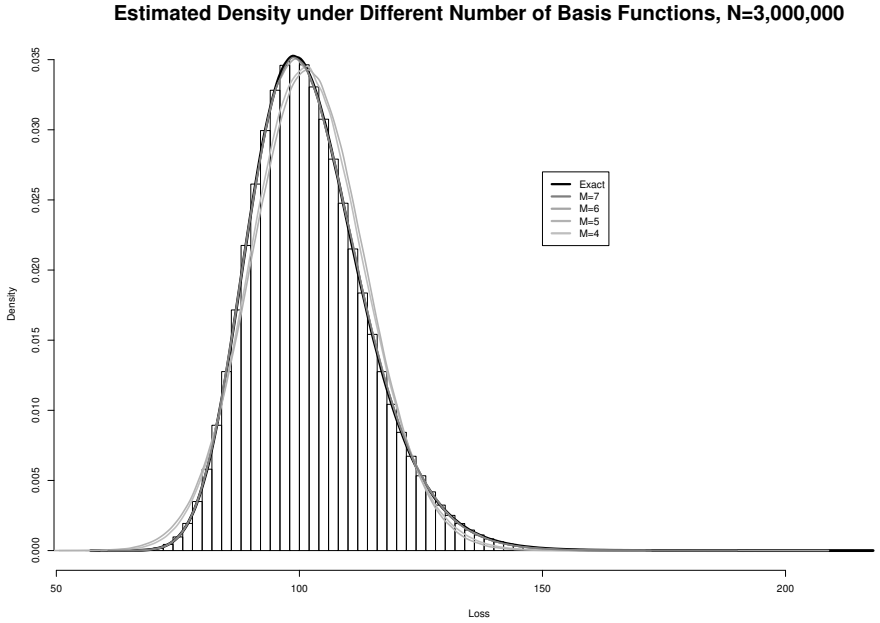

Figure 1: Empirical densities of $V(\tau)$ based on $N = 3,000,000$ Monte Carlo realizations; "exact" and using the LSM algorithm with M singular functions in the approximation.

[5]Since it is impossible to obtain the exact loss distribution at the risk horizon, we consider the estimated loss distribution obtained from the LSM algorithm with $M = 37$ monomials and $N = 40 \times 10^6$ simulations as "exact."

		$N = 100,000$		$N = 3,000,000$	
	Div.	Singular	Monomials	Singular	Monomials
$M = 4$	KS	2.52×10^{-2}	2.86×10^{-2}	2.41×10^{-2}	2.77×10^{-2}
	KL	2.17×10^{-4}	2.32×10^{-4}	2.13×10^{-4}	2.28×10^{-4}
	JS	7.43×10^{-3}	7.68×10^{-3}	7.36×10^{-3}	7.62×10^{-3}
$M = 6$	KS	7.91×10^{-3}	9.60×10^{-3}	2.24×10^{-3}	5.79×10^{-3}
	KL	1.09×10^{-5}	4.93×10^{-5}	4.53×10^{-6}	4.31×10^{-5}
	JS	1.62×10^{-3}	3.52×10^{-3}	1.06×10^{-3}	3.29×10^{-3}
$M = 12$	KS	8.28×10^{-3}	8.26×10^{-3}	1.49×10^{-3}	1.53×10^{-3}
	KL	1.43×10^{-5}	1.55×10^{-5}	6.02×10^{-7}	1.74×10^{-6}
	JS	1.84×10^{-3}	1.93×10^{-3}	3.82×10^{-4}	6.58×10^{-4}

Table 1: Statistical divergence measures between the empirical density function based on the "exact" realizations and the LSM approximation using different basis functions; mean of 300 runs with $N = 3,000,000$ sample paths each.

To assess the performance of optimal basis functions relative to naïve choices, in Table 1 we report statistical differences to the "exact" distribution according to various statistical divergence measures for singular functions and simple monomials for different numbers of simulations N and basis functions M. More precisely, the set of monomial basis functions when $M = 6$ is $(1, q_\tau, r_\tau, \mu_{x+\tau}, q_\tau^2, r_\tau^2)$, and for $M = 12$ we include all second-order terms and (q_τ^3, r_τ^3). For each combination, the table reports three common statistical divergence measures: the Kolmogorov-Smirnov statistic (KS), the Kullback-Leibler divergence (KL), and the Jensen-Shannon divergence (JS). We report the mean of three-hundred runs.

There are two general observations. First, increasing the number of basis functions M yields closer approximations of the "true" distribution. This again shows that in order to obtain a close approximation, a sufficient number of basis functions is necessary. One exception to this observation is the transition from $M = 6$ to $M = 12$ singular functions for $N = 100,000$ sample paths, where the approximation worsens. The reason is the interplay between the number of basis functions M and samples N that is emphasized in Section 3.2: The convergence rate in Proposition 3.3 is a function of M and N, and increasing M while keeping N at the same level, although yielding a closer functional approximation (second term), adversely affects the regression approximation. For the monomials, on the other hand, adding terms always decreases the divergence in Table 1, so that generally both aspects in the convergence rate are at work, with either of them dominating in some cases. We will illuminate this interplay in more detail below in the context of estimating risk measures.

The second observation is that the singular functions significantly outperform the monomials, particularly for the larger number of sample paths ($N = 3,000,000$), with a relative difference up to an order of magnitude for the KL divergence. This result documents the importance of choosing appropriate basis functions, and the virtue of singular functions as the tangible and expedient choice. This insight is even more relevant when considering that different combinations of monomials are possible – and indeed the choice in Table 1 turns out to be favorable. To illustrate, in Table 2 we present statistical divergences as well as the

	KS	KL	JS	$\text{VaR}_{99.5\%}$
Singular	2.16×10^{-3}	4.29×10^{-6}	1.04×10^{-3}	139.08
Comb. 1 (q_τ^2, r_τ^2)	5.08×10^{-3}	4.21×10^{-5}	3.25×10^{-3}	140.09
Comb. 2 (q_τ^2, $\mu_{x+\tau}^2$)	8.94×10^{-3}	2.72×10^{-5}	2.61×10^{-3}	140.56
Comb. 3 (q_τ^2, $q_\tau r_\tau$)	3.42×10^{-3}	2.96×10^{-5}	2.73×10^{-3}	139.82
Comb. 4 (q_τ^2, $q_\tau \mu_{x+\tau}$)	3.29×10^{-3}	3.22×10^{-5}	2.84×10^{-3}	139.10
Comb. 5 (q_τ^2, $r_\tau \mu_{x+\tau}$)	5.05×10^{-3}	4.29×10^{-5}	3.28×10^{-3}	140.10
Comb. 6 (r_τ^2, $\mu_{x+\tau}^2$)	2.48×10^{-2}	2.11×10^{-4}	7.33×10^{-3}	134.68
Comb. 7 (r_τ^2, $q_\tau r_\tau$)	2.50×10^{-2}	2.22×10^{-4}	7.52×10^{-3}	134.56
Comb. 8 (r_τ^2, $q_\tau \mu_{x+\tau}$)	3.72×10^{-2}	2.09×10^{-4}	7.29×10^{-3}	132.34
Comb. 9 (r_τ^2, $r_\tau \mu_{x+\tau}$)	2.88×10^{-2}	2.27×10^{-4}	7.60×10^{-3}	133.80
Comb. 10 ($\mu_{x+\tau}^2$, $q_\tau r_\tau$)	2.17×10^{-2}	2.07×10^{-4}	7.25×10^{-3}	135.26
Comb. 11 ($\mu_{x+\tau}^2$, $q_\tau \mu_{x+\tau}$)	3.35×10^{-2}	1.95×10^{-4}	7.05×10^{-3}	133.07
Comb. 12 ($\mu_{x+\tau}^2$, $r_\tau \mu_{x+\tau}$)	2.47×10^{-2}	2.11×10^{-4}	7.33×10^{-3}	134.59
Comb. 13 ($q_\tau r_\tau$, $q_\tau \mu_{x+\tau}$)	3.37×10^{-2}	2.05×10^{-4}	7.23×10^{-3}	132.99
Comb. 14 ($q_\tau r_\tau$, $r_\tau \mu_{x+\tau}$)	2.50×10^{-2}	2.23×10^{-4}	7.54×10^{-3}	134.44
Comb. 15 ($q_\tau \mu_{x+\tau}$, $r_\tau \mu_{x+\tau}$)	3.65×10^{-2}	2.08×10^{-4}	7.28×10^{-3}	132.40

Table 2: Statistical divergence measures between the empirical density function based on the "exact" realizations and the LSM approximation using different basis functions with $M = 6$, and VaR at 99.5%; mean of 300 runs with $N = 3,000,000$ sample paths each. C1 to C15 are based on simple monomials.

99.5% VaR for $M = 6$ singular functions as well as for 15 different possible combinations of six monomials, where in addition to the first-order terms for each of the state variables we include all possible combinations of two second-order terms. We again report the mean of three-hundred runs based on $N = 3,000,000$ samples,[6] whereas Figure 2 provides corresponding box-and-whisker plots of the outcomes.[7]

Again, we find that singular functions – as the optimal choice – significantly outperform all combinations of monomials, and the differences can be drastic. Specifically, while combinations 1 through 5 come somewhat close to the results from singular functions at least in view of the KS metric and the estimated VaR, combinations 6 through 15 perform an order of magnitude worse. It is interesting to note that the component missing in combinations 6-15 is the square of the log-price of the risky asset q_τ. This illustrates the relevance of non-linear effects in q_τ with respect to the value of the liability. The box-and-whisker plots in Figure 2 reveal that across the entire domain of the distribution (which is relevant to the KL and JS divergences), the singular functions perform considerably better than *any* of the monomial combinations. This is still the case for the KS divergence, although here differences are less

[6]To not bias the results, we use different random numbers for Tables 1 and 2, so that sampling error explains small differences in the tables as well as some of the observations within each table (e.g., the order of the KS results for $M = 12$ in Table 1).

[7]Here and in what follows, the box presents the area between the first and third quartile, with the inner line placed at the median; the whisker line spans samples that are located closer than 150% of the interquartile range to the upper and lower quartiles, respectively (Tukey box-and-whisker plot).

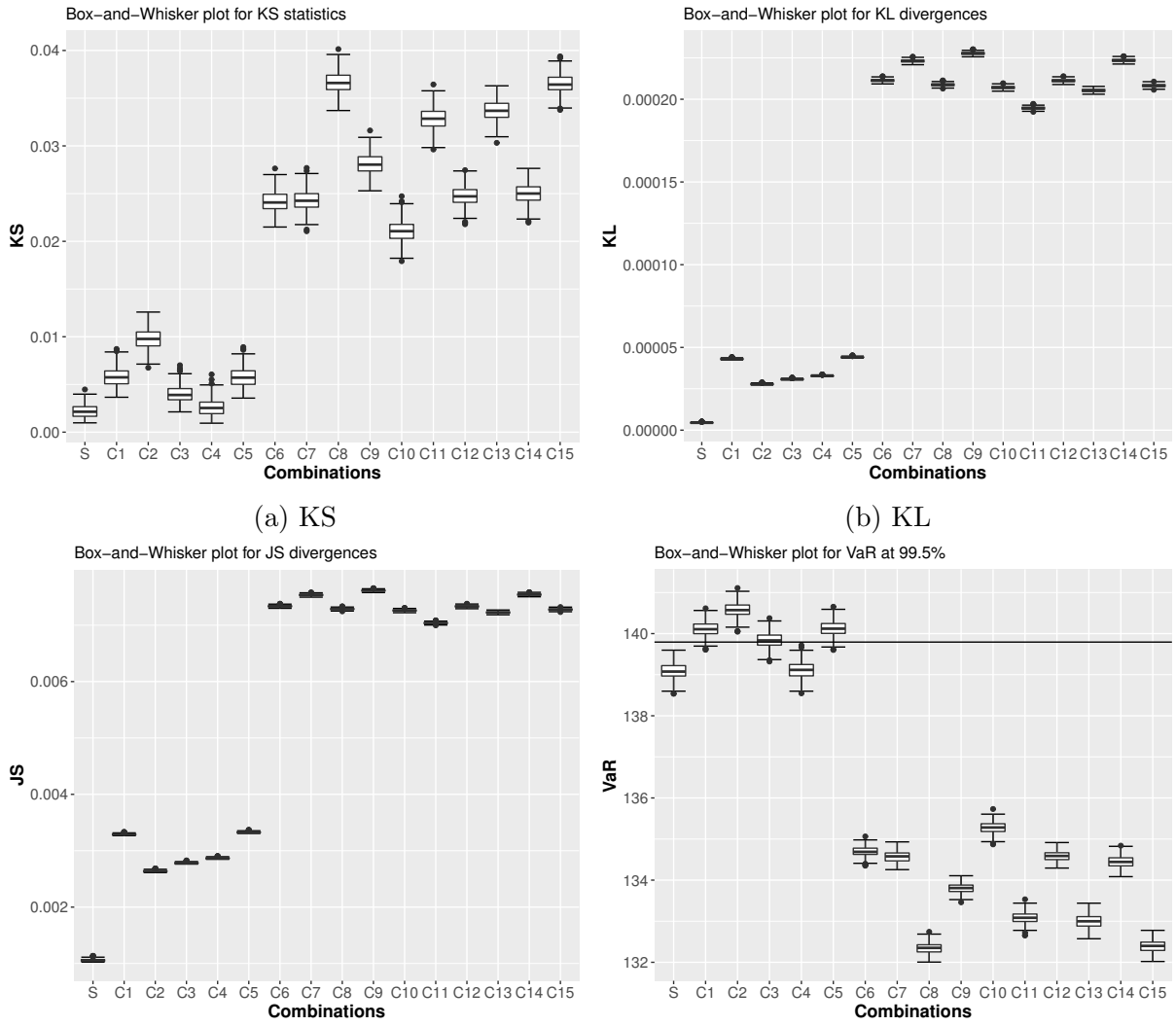

(a) KS

(b) KL

(c) JS

(d) VaR at 99.5%

Figure 2: Box-and-whisker plots for various statistical divergence measures and 99.5% VaR calculated using the LSM algorithm with different basis functions with $M = 6$; based on 300 runs with $N = 3,000,000$ sample paths each. C1 to C15 are based on simple monomials. Cf. Table 2.

		$\underline{b} = 0.95b$		$\bar{b} = 1.05b$	
	Div.	Singular	Monomials	Singular	Monomials
$M = 4$	KS	2.71×10^{-2}	2.98×10^{-2}	2.16×10^{-2}	2.59×10^{-2}
	KL	2.25×10^{-4}	2.39×10^{-4}	1.98×10^{-4}	2.14×10^{-4}
	JS	7.58×10^{-3}	7.80×10^{-3}	7.10×10^{-3}	7.38×10^{-3}
	$Q_{1,\text{VaR}}$	132.17	131.66	137.02	136.22
	$Q_{3,\text{VaR}}$	132.31	131.80	137.18	136.36
$M = 6$	KS	2.48×10^{-3}	5.90×10^{-3}	1.99×10^{-3}	4.94×10^{-3}
	KL	4.61×10^{-6}	4.27×10^{-5}	4.43×10^{-6}	4.31×10^{-5}
	JS	1.07×10^{-3}	3.27×10^{-3}	1.05×10^{-3}	3.29×10^{-3}
	$Q_{1,\text{VaR}}$	137.09	138.10	140.99	141.99
	$Q_{3,\text{VaR}}$	137.34	138.35	141.26	142.25
$M = 12$	KS	1.64×10^{-3}	1.70×10^{-3}	1.46×10^{-3}	1.58×10^{-3}
	KL	5.99×10^{-7}	1.56×10^{-6}	5.97×10^{-7}	1.57×10^{-6}
	JS	3.79×10^{-4}	6.22×10^{-4}	3.79×10^{-4}	6.26×10^{-4}
	$Q_{1,\text{VaR}}$	137.77	137.85	141.65	141.76
	$Q_{3,\text{VaR}}$	138.15	138.26	142.03	142.12

Table 3: Statistical divergence measures between the empirical density function based on the "exact" realizations and the LSM approximation using different basis functions; mean of 300 runs with $N = 3,000,000$ sample paths each. $Q_{1,\text{VaR}}$ and $Q_{3,\text{VaR}}$ are the first and third quartile of the distribution of the 99.5% VaR.

pronounced. In particular, sample error here may render an arbitrary realization under C4 or C5 to be better than an arbitrary realization under the singular function approximation. This is also true for the VaR estimate as is evident from panel (d) in Figure 2, where the horizontal line at 139.74 depicts the "exact" VaR.

Before we move on to analyzing the results for VaR in more detail, we note that our findings with regards to the superior performance of the singular functions are not driven by the specific payoff function: As discussed in detail in Section 4, our notion of *optimality* is tied to the *model framework* rather than a specific cash flow *model*. To illustrate, Table 3 shows results for different basis functions for different payoffs, where we modify the guaranteed annuity payment b in the payoff definition (14). More precisely, we show results for a less generous contract where we decrease the annuity by 5% ($\underline{b}$) and a more generous contract where we increase the annuity by 5% ($\bar{b}$). In addition to the statistical divergences as in Table 1, we also report the first and third quartiles of 300 VaR estimates based on different sample paths. The estimated "exact" 99.5% VaR when using $\underline{b}$ is 137.89, and the "exact" 99.5% VaR for $\bar{b}$ is 141.79. The results are analogous: Singular functions perform better than monomials, and the difference can be substantial for $M = 6$ and 12.

Risk measure estimation.

One of the key take-aways from the foregoing analyses is that a significant number of basis functions M is necessary to obtain an accurate approximation to the capital distribution.

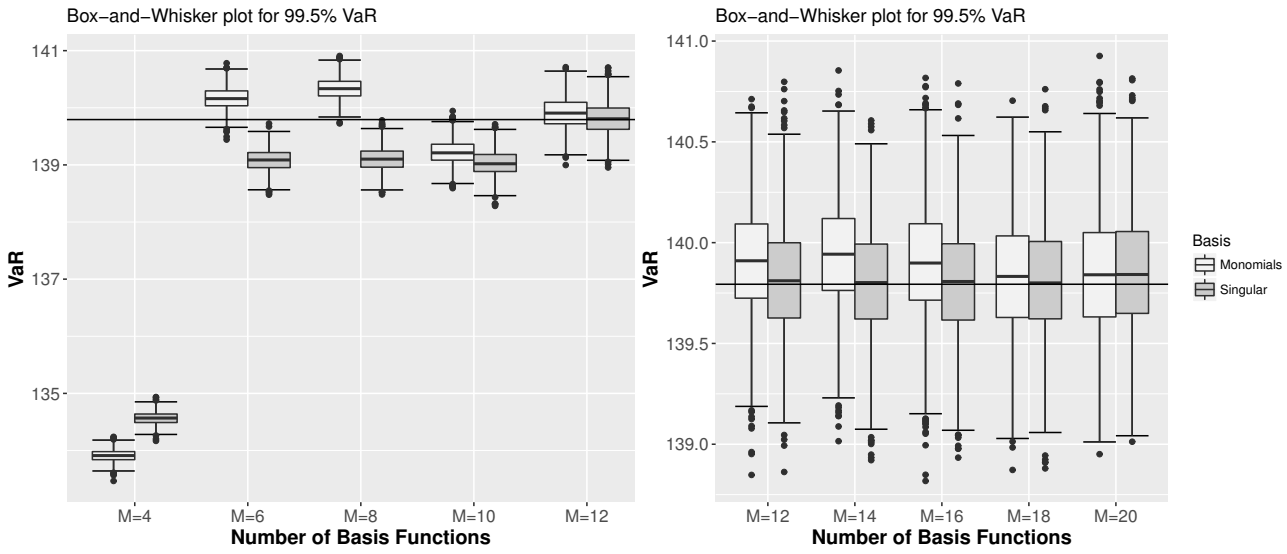

(a) small M (b) large M

Figure 3: Box-and-whisker plots for 99.5% VaR calculated using the LSM algorithm with different numbers of basis functions M; based on 1,500 runs with $N = 3,000,000$ sample paths each.

For instance, panel (d) in Figure 2 shows that the "exact" VaR estimate lies outside the whiskers for the singular value functions as well as for most of the monomial combinations – and significantly so for combinations 6 through 15. Similarly, the "exact" VaR estimates of 137.89 and 141.79 for an annuity payment of $\underline{b}$ and $\bar{b}$ (Table 3) are outside of the first to third quartile for $M = 4$ and 6. To illustrate this relationship in more detail, Figure 3 gives box-and-whisker plots for different numbers of basis functions M – both singular functions and monomials – based on 1,500 runs of $N = 3,000,000$ sample paths each.

The left-hand panel (a) shows that obtaining a good approximation for the distribution tail is not possible for limited M and, indeed, the pattern is erratic for the monomials: While the box-and-whisker plot for $M = 6$ suggests a decent prediction, the situation worsens for $M = 10$ and the "exact" VaR estimate now lies outside the whiskers. In contrast, the pattern is more systematic for the singular functions as the different (orthogonal) dimensions are addressed sequentially. For $M = 12$ basis functions, the functional approximation is sufficiently accurate even in this tail region, and adding additional basis function does not improve on the central estimate – at least for the singular functions (right-hand panel (b) of Figure 3). Again, we notice that the pattern for the monomials is slightly erratic so that we can conclude that, for VaR estimation also, singular functions perform superior as long as we rely on a sufficient number M.

As a second observation, even for $N = 3,000,000$ sample paths, the results between the different simulation runs vary considerably. For instance, for $M = 12$ and singular functions, the whiskers based on the different runs span roughly 139.1 to 140.5, so the lengths is 1.4 or roughly 1% of the central estimate. Given the usual scale of capital requirements in the financial services industry, the cost for an additional percent of required capital is substantial. And, in fact, the whisker plots become wider as the number of basis functions increases

(roughly $[139, 140.7]$ for $M = 20$). This originates from the interplay between the number of basis functions M and the number of simulations N mentioned above.

To illustrate this interplay in more detail, Figure 4 replots Figure 3b for singular functions, but varying the number of underlying simulations N used in each run. We find that for a limited number of simulation paths N, the mentioned effects are more pronounced. Specifically, for $N = 100,000$ the length of the whisker plot amounts to more than 5% of the central estimate and it increases as the number of basis functions M increases. We also notice a bias in the central estimate for $M = 18$ and $M = 20$, which is a manifestation of the result from Proposition 3.4 – although, as discussed there, the bias is overshadowed by the sample variance resulting from the Monte Carlo estimation.

This tradeoff between the number of basis functions M and the number of simulation paths N is also a primary reason of why the choice of basis functions is material. Since N will have to grow as M increases, given a fixed computational budget, feeding the algorithm with a very large number of basis functions will be futile. With a limited number of simulations but a large number of basis functions, the regression approximation will over-fit spurious patterns in the simulated data. While navigating this bias-variance tradeoff is a familiar problem in the statistical learning context (Hastie et al., 2009), we note that conventional mitigation techniques such as regularization do not trivially resolve this difficulty.

To illustrate, we repeat our VaR estimations for $M = 16$ basis functions – using both, singular functions and monomials – where instead of OLS, we employ ridge regression to fit the approximation.[8] We choose the regularization parameter based on 10-fold cross-validation. Figure 5 displays box-and-whisker plots for the 99.5% VaR for $N = 50,000$ sample paths (left-hand panel (a)) and $N = 3,000,000$ sample paths (right-hand panel (b)), using both singular functions and monomials as the basis functions.

Comparing the results to the VaR estimates from Figure 3b, we find that relying on a regularized regression can be precarious. More precisely, while the box-and-whisker plot for the singular functions approximation in the case $N = 50,000$ seems to be roughly in line with the results from Figure 4, the plot when using monomials as basis functions – while notably tighter – now significantly undershoots and it no longer includes the "exact" VaR. The findings for $N = 3,000,000$ are similar, although now here the "exact" VaR is outside the whiskers also for the singular basis functions.

To provide intuition for these results, Figure 6 plots effective degrees of freedom (EDF) for the fits underlying Figure 5 (we refer to Hastie et al. (2009) for the definition of EDF in ridge regression). We notice that EDFs are very close to 15 for the singular functions, both for $N = 50,000$ and $N = 3,000,000$ (Panels (a) and (b)). Since 16 basis functions correspond exactly to 15 degrees of freedom (the constant term is always included), the shrinkage coming from the regularization is relatively minor – although it is clear from Figure 5b that the effect is still significant enough to move the VaR estimates downward. In contrast, for the monomial basis functions, the EDFs are around 10.9 and 13.25 for $N = 50,000$ and $N = 3,000,000$, respectively, so that here the shrinkage is substantial (Panels (c) and (d)) – explaining both the compression and the shifting of the box-and-whisker plots.

Since the regularization parameter is chosen so as to minimize the mean-squared pre-

[8] The ridge regression coefficients, $\alpha_{ridge}^{(N)}$, minimize the sum of squares plus a regularization term $\eta \sum_{k=2}^{M} \alpha_k^2$, where η is a regularization parameter. We assume that the first basis function is always constant.

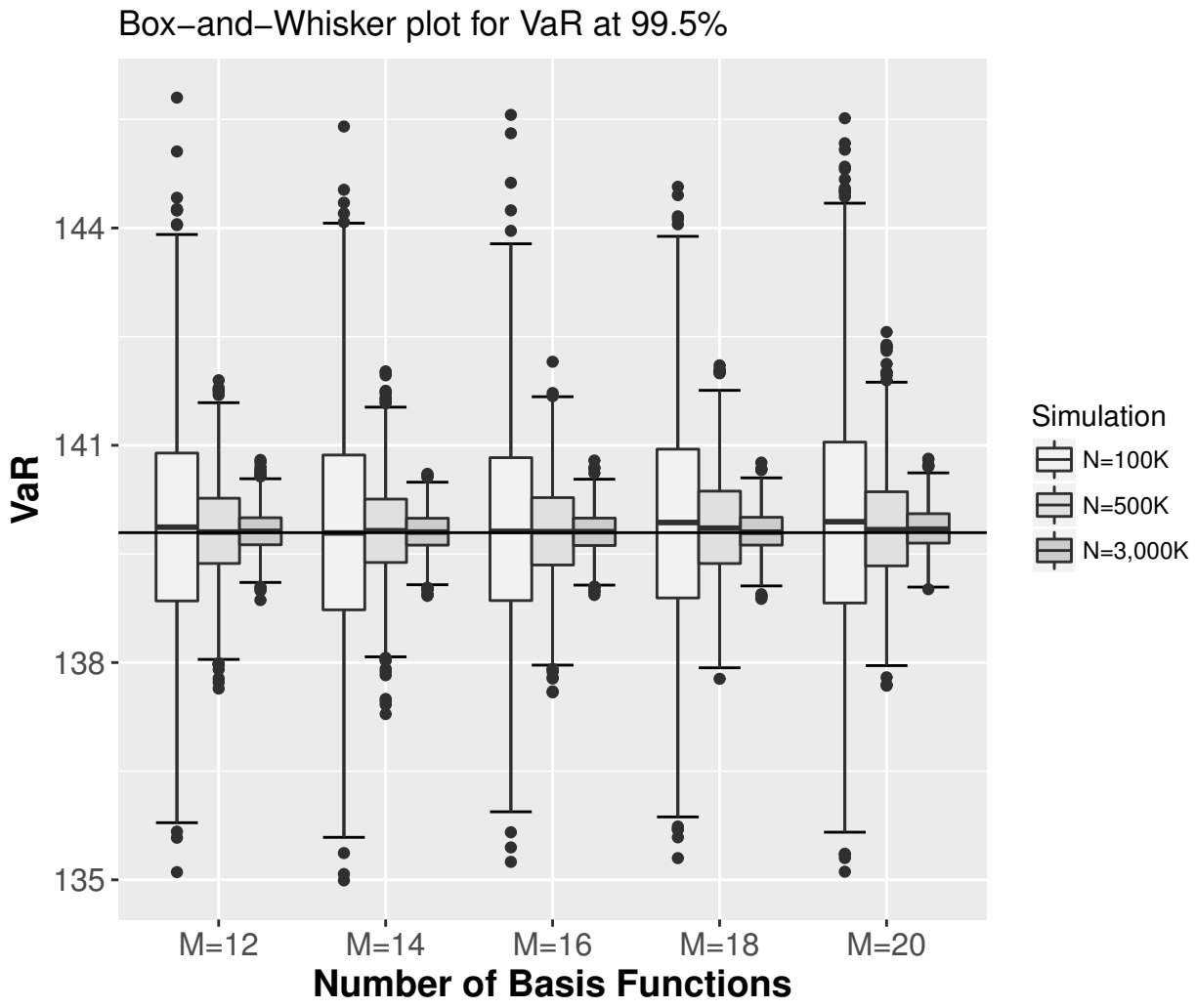

Figure 4: Box-and-whisker plots for 99.5% VaR calculated using the LSM algorithm with different number of simulations ($N = 100,000$, $N = 500,000$, and $N = 3,000,000$) and different numbers of basis functions M; based on 1,500 runs. All figures are produced using singular functions.

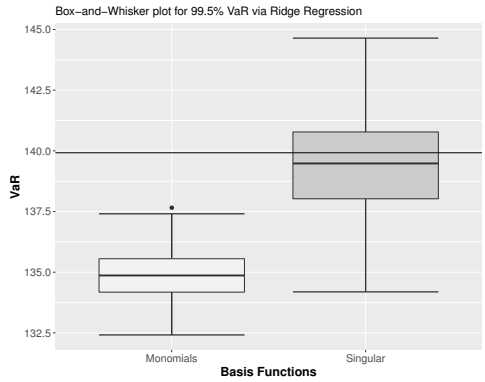

(a) $N = 50,000$

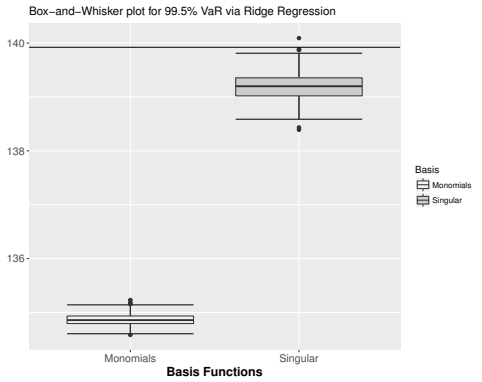

(b) $N = 3,000,000$

Figure 5: Box-and-whisker plots for VaR at 99.5% calculated using the LSM algorithm with ridge regression to fit parameters with different basis functions ($M = 16$) and different numbers of simulations N; based on 300 runs.

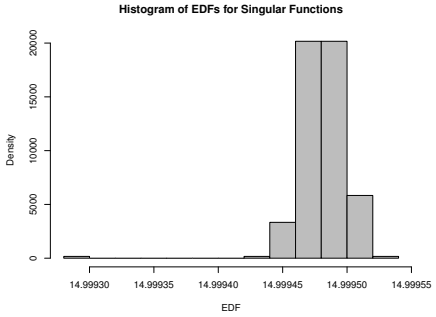

(a) $N = 50,000$, Singular Functions

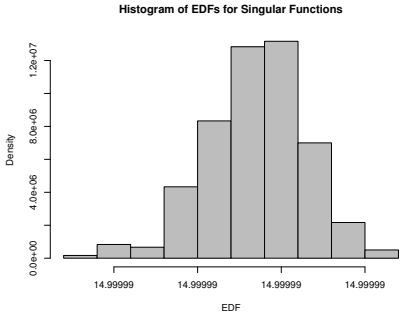

(b) $N = 3,000,000$, Singular Functions

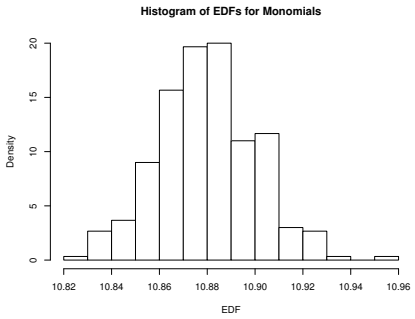

(c) $N = 50,000$, Monomials

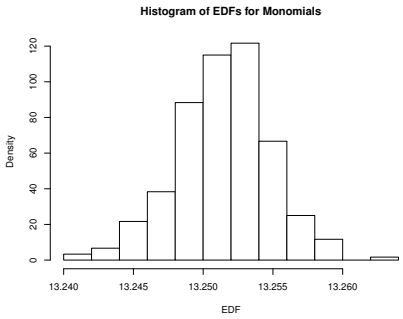

(d) $N = 3,000,000$, Monomials

Figure 6: Histograms of EDFs for the ridge regression with singular functions and monomials using $M = 16$ basis functions and different numbers of simulations N; based on 300 runs.

diction error across all realizations, it is not surprising that the predictions worsen in a certain area of the distribution. Indeed, it appears that the incurred bias for gains in terms of variance has an adverse effect for estimating VaR. For the singular functions, while the impact on the VaR estimate is limited, this is because overall there is very little change in the estimates relative to OLS – whereas for the monomial basis functions, the estimates are zooming in on the wrong target.

6 Conclusion

We discuss a Least-Squares Monte Carlo (LSM) algorithm for estimating financial capital in *nested* valuation settings. The algorithm relies on functional approximations of conditional expected values and least-squares regression. After establishing the algorithm, we analyze convergence of the approach and examine properties when estimating VaR. Moreover, we discuss the choice of basis functions in the functional approximation. Specifically, we show that the left singular functions of the valuation operator that maps cash flows to capital present *optimal* basis functions for a model framework. We derive optimal basis functions in settings where the underlying Markov state variable follows a Gaussian distribution, and we apply our ideas in a relevant example from life insurance.

Our numerical illustrations document that the algorithm can provide viable results at relatively low computational costs (compared to, e.g., nested simulations). The algorithm, therefore, provides one potential solution to pressing practical problems such as the calculation of capital requirements in life insurance according to the recent Solvency II directive. Two key insights emerge from our analyses in view of applying the LSM algorithm in practical settings. First, increasing the number of basis functions comes at a cost since it is necessary to simultaneously increase the number of simulations N, and finessing the tradeoff is not trivial. Second, in multivariate settings, a key issue is not only choosing the functional class of basis functions – which appears less crucial in our exercises – but rather the combinations of basis functions that are important for spanning the payoff space in view of valuation. Even in the three-dimensional setting considered here, this is of critical importance as naïve choices may yield significantly worse results. The choice of basis functions will become even more important as the complexity and the dimensionality of the problem increase, as it is the case in practical applications.

Various extensions are possible. One aspect that is particularly interesting is tailoring the approach to the evaluation of tail risk measures, to boost its performance when estimating VaR or ES.

References

Abbe, E., Zheng, L., 2012. A coordinate system for Gaussian networks. IEEE Transactions on Information Theory, 58: 721-733.

Amemiya, T., 1985. Advanced econometrics. Harvard university press, Cambridge.

Barrie and Hibbert, 2011. "A Least Squares Monte Carlo Approach to Liability Proxy

Modelling and Capital Calculation" by A. Koursaris. Available at http://www.barrhibb.com.

Bauer, D., Benth, F.E., Kiesel, R., 2012b. Modeling the forward surface of mortality. SIAM Journal on Financial Mathematics, 3: 639-666.

Bauer, D., Bergmann, D., Reuss, A., 2010. Solvency II and Nested Simulations – a Least-Squares Monte Carlo Approach. Paper presented at the International Congress of Actuaries 2010. Available at http://www.africanagenda.com/ica2010/.

Bauer, D., Reuss, A., Singer, D., 2012b. On the Calculation of the Solvency Capital Requirement based on Nested Simulations. ASTIN Bulletin, 42: 453-499.

Bauer, D., Zanjani, G., 2016. The marginal cost of risk, risk measures, and capital allocation. Management Science, 62: 1431-1457.

Benedetti, G., 2017. On The Calculation Of Risk Measures Using Least-Squares Monte Carlo. International Journal of Theoretical and Applied Finance, 20.

Beutner, E., Pelsser, A., and Schweizer, J., 2013. Fast convergence of Regress-Later estimates in Least Squares Monte Carlo. Working Paper available on arXiv, arXiv:1309.5274.

Birman, M.S., Solomyak, M.Z., 1977. Estimates of singular numbers of integral operators. Russian Mathematical Surveys, 32: 15-89.

Breiman, L., Friedman, J.H., 1985. Estimating optimal transformations for multiple regression and correlation. Journal of the American Statistical Association, 80: 580-598.

Brigo, D., Mercurio, F., 2006. Interest rate models – Theory and Practice with Smile, Inflation and Credit. Second Edition. Springer, Berlin.

Broadie, M., Du, Y., Moallemi, C.C, 2015. Efficient risk estimation via nested sequential simulation. Management Science, 57: 1172-1194.

Broadie, M., Du, Y., Moallemi, C.C, 2015. Risk Estimation via Regression. Operations Research, 63: 1077-1097.

Cambou, M., Filipović, D., 2018. Replicating Portfolio Approach to Capital Calculation. Finance and Stochastics, 22: 181-203.

Carriere, J.F., 1996. Valuation of the early-exercise price for options using simulations and nonparametric regression. Insurance: Mathematics and Economics, 19: 19-30.

Chen, X., Nelson, B.L., Kim, K.K., 2012. Stochastic kriging for conditional value-at-risk and its sensitivities. Proceedings of the 2012 Winter Simulation Conference, IEEE.

Clément, E., Lamberton, D., Protter, P., 2002. An analysis of a least squares regression method for american option pricing. Finance and Stochastics, 6: 449-471.

DAV, 2015. Proxy-Modelle für die Risikokapitalberechnung. Technical Report, Ausschuss Investment der Deutschen Aktuarvereinigung, e.V. (DAV).

Floryszczak A., Le Courtois O., Majri M., 2016. Inside the Solvency 2 Black Box: Net Asset Values and Solvency Capital Requirements with a Least-Squares Monte-Carlo Approach. Insurance: Mathematics and Economics, 71: 15-26.

Glasserman, P., 2004. Monte Carlo Methods in Financial Engineering. Springer, New York.

Glasserman, P., Heidelberger, P., Shahabuddin, O., 2000. Variance reduction techniques for estimating value-at-risk. Management Science, 46: 1349-1364.

Glasserman, P., Yu, B., 2002. Simulation for American options: regression now or regression later? In Monte Carlo and Quasi-Monte Carlo Methods, 213-226, Springer, Berlin.

Gordy, M.B., Juneja, S., 2010. Nested simulations in portfolio risk measurement. Management Science, 56: 1833-1848.

Ha, H., 2016. Essays on Computational Problems in Insurance. Dissertation, Georgia State University. `https://scholarworks.gsu.edu/rmi_diss/40`.

Hastie, T., Tibshirani, R., Friedman, J., 2009. The Elements of Statistical Learning – Data Mining, Inference, and Prediction, Second Edition. Springer, New York.

Hong, L.J., Juneja, S., Liu, G., 2017. Kernel smoothing for nested estimation with application to portfolio risk measurement. Operations Research, 65: 657-673.

Huang, Q., 2012. Some Topics Concerning the Singular Value Decomposition and Generalized Singular Value Decomposition. Ph.D. thesis, Arizona State University

Kaina, M., Rüschendorf, L., 2009. On convex risk measures on L^p-spaces. Mathematical Methods of Operations Research, 69: 475-495.

Khare, K., Zhou, H., 2009. Rate of Convergence of Some Multivariate Markov Chains with Polynomial Eigenfunctions. The Annals of Applied Probability, 19: 737-777.

Kollo, T., Rosen, D.V., 2006. Advanced multivariate statistics with matrices. Springer, New York.

Lan, H., Nelson, B.L., Staum, J., 2010. A confidence interval procedure for expected shortfall risk measurement via two-level simulation. Operations Research, 58: 1481-1490.

Lee, S.-H., 1998. Monte Carlo computation of conditional expectation quantities. Ph.D. thesis, Stanford University.

Linetsky, V., 2004. The spectral decomposition of the option value. International Journal of Theoretical and Applied Finance, 7: 337-384.

Liu, M., Staum, J., 2010. Stochastic kriging for efficient nested simulation of expected shortfall. The Journal of Risk, 12: 3-27.

Longstaff, F.A., Schwartz, E.S., 2001. Valuing American Options by Simulation: A Simple Least-Squares Approach. Review of Financial Studies, 14: 113-147.

Makur, A., Zheng, L., 2016. Polynomial spectral decomposition of conditional expectation operators. 54th Annual Allerton Conference Communication, Control, and Computing (pp. 633-640). IEEE.

Milliman, 2013. "Least Squares Monte Carlo for fast and robust Capital projections" by C. Bettels, F. Ketterer, M. Hoerig, and M. Leitschkis. Available at `http://us.milliman.com`.

Moreno, M., Navas, J.F., 2003. On the Robustness of Least-Squares Monte Carlo (LSM) for Pricing American Derivatives. Review of Derivatives Research, 14: 113-147.

Natolski, J., Werner, R., 2017. Mathematical foundation of the replicating portfolio approach. Scandinavian Actuarial Journal, forthcoming.

Newey, W.K., 1997. Convergence rates and asymptotic normality for series estimators. Journal of Econometrics, 79: 147-168.

Pelsser, A., Schweizer, J., 2016. The Difference between LSMC and Replicating Portfolio in Insurance Liability Modeling. European Actuarial Journal, 6: 441-494.

Risk, J., Ludkovski, M., 2017. Sequential Design and Spatial Modeling for Portfolio Tail Risk Measurement. Working paper available on arXiv, arXiv:1710.05204.

Serdyukov A.S., Patutin A.V., Shilova T.V., 2014. Numerical Evaluation of the Truncated Singular Value Decomposition Within the Seismic Traveltimes Tomography Framework. Journal of Siberian Federal University. Mathematics and Physics, 7: 208-218.

Tsitsiklis, J.N., Van Roy, B., 2001. Regression methods for pricing complex American-style options. IEEE Transactions on Neural Networks, 12: 694-763.

Vasicek, O., 1997. An Equilibrium Characterization of the Term Structure. Journal of Financial Economics, 5: 177-188.

Weber, S., 2007. Distribution-Invariant Risk Measures, Entropy, and Large Deviations. Journal of Applied Probability, 44: 16-40.

Whitt, W., 1986. Stochastic comparisons for non-Markov processes. Mathematics of Operations Research, 11: 608-618.

Zhu, N., Bauer, D., 2011. Applications of Forward Mortality Factor Models in Life Insurance Practice. The Geneva Papers on Risk and Insurance, 36: 567-594

Appendix

A Proofs

Proof of Lemma 2.1. 1. Let $A \in \mathcal{F}_t,\ 0 \le t \le \tau$. Then:

$$\begin{aligned}\tilde{\mathbb{P}}(A) &= \mathbb{E}^{\tilde{\mathbb{P}}}[\mathbf{1}_A] = \mathbb{E}^{\mathbb{P}}\left[\frac{\partial\tilde{\mathbb{P}}}{\partial\mathbb{P}}\mathbf{1}_A\right] = \mathbb{E}^{\mathbb{P}}\left[\mathbb{E}^{\mathbb{P}}\left[\frac{\frac{\partial\mathbb{Q}}{\partial\mathbb{P}}}{\mathbb{E}^{\mathbb{P}}\left[\frac{\partial\mathbb{Q}}{\partial\mathbb{P}}\,|\mathcal{F}_\tau\right]}\mathbf{1}_A\middle|\mathcal{F}_\tau\right]\right] \\ &= \mathbb{E}^{\mathbb{P}}\left[\frac{\mathbf{1}_A}{\mathbb{E}^{\mathbb{P}}\left[\frac{\partial\mathbb{Q}}{\partial\mathbb{P}}\,|\mathcal{F}_\tau\right]}\mathbb{E}^{\mathbb{P}}\left[\frac{\partial\mathbb{Q}}{\partial\mathbb{P}}\middle|\mathcal{F}_\tau\right]\right] = \mathbb{P}(A).\end{aligned}$$

2. Let $X : \Omega \to \mathbb{R}$ be a random variable. Then:

$$\begin{aligned}\mathbb{E}^{\tilde{\mathbb{P}}}[X\,|\mathcal{F}_\tau] &= \underbrace{\frac{1}{\mathbb{E}^{\mathbb{P}}\left[\frac{\partial\tilde{\mathbb{P}}}{\partial\mathbb{P}}\,|\mathcal{F}_\tau\right]}}_{=1}\mathbb{E}^{\mathbb{P}}\left[\frac{\partial\tilde{\mathbb{P}}}{\partial\mathbb{P}}X\middle|\mathcal{F}_\tau\right] = \mathbb{E}^{\mathbb{P}}\left[\frac{X\frac{\partial\mathbb{Q}}{\partial\mathbb{P}}}{\mathbb{E}^{\mathbb{P}}\left[\frac{\partial\mathbb{Q}}{\partial\mathbb{P}}\,|\mathcal{F}_\tau\right]}\middle|\mathcal{F}_\tau\right] \\ &= \frac{1}{\mathbb{E}^{\mathbb{P}}\left[\frac{\partial\mathbb{Q}}{\partial\mathbb{P}}\,|\mathcal{F}_\tau\right]}\mathbb{E}^{\mathbb{P}}\left[\frac{\partial\mathbb{Q}}{\partial\mathbb{P}}X\middle|\mathcal{F}_\tau\right] = \mathbb{E}^{\mathbb{Q}}[X|\,\mathcal{F}_\tau].\end{aligned}$$

□

Proof of Lemma 2.2. Linearity is obvious. For the proof of continuity, consider a sequence $h^{(n)} \to h \in \mathcal{H}$. Then:

$$\begin{aligned}&\mathbb{E}^{\mathbb{P}}\left[L\,h^{(n)} - L\,h\right]^2 \\ =\ &\mathbb{E}^{\mathbb{P}}\left[\left(\sum_{j=\tau}^{T}\mathbb{E}^{\tilde{\mathbb{P}}}\left[\left(h_j^{(n)} - h_j\right)(Y_j)\,|Y_\tau\right]\right)^2\right] \\ =\ &\mathbb{E}^{\mathbb{P}}\left[\sum_{j,k}\mathbb{E}^{\tilde{\mathbb{P}}}\left[\left(h_j^{(n)} - h_j\right)(Y_j)\,|Y_\tau\right]\mathbb{E}^{\tilde{\mathbb{P}}}\left[\left(h_k^{(n)} - h_k\right)(Y_k)\,|Y_\tau\right]\right] \\ \le\ &\sum_{j,k}\sqrt{\mathbb{E}^{\mathbb{P}}\left[\left(\mathbb{E}^{\tilde{\mathbb{P}}}\left[\left(h_j^{(n)} - h_j\right)(Y_j)\,|Y_\tau\right]\right)^2\right]}\times\sqrt{\mathbb{E}^{\mathbb{P}}\left[\left(\mathbb{E}^{\tilde{\mathbb{P}}}\left[\left(h_k^{(n)} - h_k\right)(Y_k)\,|Y_\tau\right]\right)^2\right]} \\ \le\ &\sum_{j,k}\sqrt{\mathbb{E}^{\tilde{\mathbb{P}}}\left[\left(h_j^{(n)} - h_j\right)^2(Y_j)\right]}\times\sqrt{\mathbb{E}^{\tilde{\mathbb{P}}}\left[\left(h_k^{(n)} - h_k\right)^2(Y_k)\right]} \to 0,\ n\to\infty,\end{aligned}$$

where we used the Cauchy-Schwarz inequality, the conditional Jensen inequality, and the tower property of conditional expectations. □

Proof of Lemma 2.3. Consider the operator $L^{(j)}$ mapping from $L^2(\mathbb{R}^d, \mathcal{B}, \tilde{\mathbb{P}}_{Y_j})$ to $L^2(\mathbb{R}^d, \mathcal{B}, \mathbb{P}_{Y_\tau})$. Since $L^{(j)}$ is the (conditional) expectation under the assumption that there exists a joint density, it can be represented as:

$$\begin{aligned} L^{(j)}\,\mathbf{x} &= \int_{\mathbb{R}^d} \mathbf{x}(y)\,\pi_{Y_j|Y_\tau}(y|x)\,dy = \int_{\mathbb{R}^d} \mathbf{x}(y)\frac{\pi_{Y_\tau,Y_j}(x,y)}{\pi_{Y_\tau}(x)}\,dy \\ &= \int_{\mathbb{R}^d} \mathbf{x}(y)\frac{\pi_{Y_\tau,Y_j}(x,y)}{\pi_{Y_j}(y)\pi_{Y_\tau}(x)}\pi_{Y_j}(y)\,dy = \int_{\mathbb{R}^d} \mathbf{x}(y)\,k(x,y)\,\pi_{Y_j}(y)\,dy, \end{aligned}$$

where $\mathbf{x}$ is an element of $L^2(\mathbb{R}^d, \mathcal{B}, \tilde{\mathbb{P}}_{Y_j})$, $\pi_{Y_j}(y)$ and $\pi_{Y_\tau}(x)$ are marginal density functions for Y_j and Y_τ in $L^2(\mathbb{R}^d, \mathcal{B}, \tilde{\mathbb{P}}_{Y_j})$ and $L^2(\mathbb{R}^d, \mathcal{B}, \mathbb{P}_{Y_\tau})$, respectively, and $k(x,y) = \frac{\pi_{Y_\tau,Y_j}(x,y)}{\pi_{Y_j}(y)\pi_{Y_\tau}(x)}$. Thus, $L^{(j)}$ is an integral operator with kernel $k(x,y)$. Moreover:

$$\int_{\mathbb{R}^d}\int_{\mathbb{R}^d} |k(x,y)|^2\,\pi_{Y_j}(y)\pi_{Y_\tau}(x)\,dy\,dx = \int_{\mathbb{R}^d}\int_{\mathbb{R}^d} \pi_{Y_j|Y_\tau}(y|x)\,\pi_{Y_\tau|Y_j}(x|y)\,dy\,dx < \infty.$$

Thus, $L^{(j)}$ is a Hilbert-Schmidt operator (e.g. Prop. VI.6.3 in Werner (2005)), and therefore compact. Finally, L is the sum of $L^{(j)}$, $j = \tau, ..., T$, and therefore also compact. □

Proof of Proposition 3.1. $\mathbb{P}_{Y_\tau}$ is a regular Borel measure as a finite Borel measure and hence $L^2\left(\mathbb{R}^d, \mathcal{B}, \mathbb{P}_{Y_\tau}\right)$ is separable (see Proposition I.2.14 and p. 33 in Werner (2005)). Now if $\{e_k,\ k = 1, 2, \ldots, M\}$ are independent, by Gram-Schmidt we can find an orthonormal system $S = \{f_k,\ k = 1, 2, \ldots, M\}$ with $\operatorname{lin}\{e_k,\ k = 1, 2, \ldots, M\} = \operatorname{lin} S$. For S, on the other hand, we can find an orthonormal basis $\{f_k,\ k \in \mathbb{N}\} = S' \supset S$. Hence:

$$\widehat{C}_\tau^{(M)} = \sum_{k=1}^{M} \alpha_k\,e_k = \sum_{k=1}^{M} \underbrace{\tilde{\alpha}_k}_{\langle C_\tau, f_k\rangle}\ f_k \to \sum_{k=1}^{\infty} \tilde{\alpha}_k\,f_k = C_\tau,\ M \to \infty,$$

where:

$$\left\|\widehat{C}_\tau^{(M)} - C_\tau\right\|^2 = \sum_{k=M+1}^{\infty} |\langle C_\tau, f_k\rangle|^2 \to 0,\ M \to \infty,$$

by Parseval's identity.

For the second part, we note that:

$$(\hat{\alpha}_1^{(N)}, \ldots, \hat{\alpha}_M^{(N)})' = \hat{\alpha}^{(N)} = \left(A^{(M,N)}\right)^{-1} \frac{1}{N}\sum_{i=1}^{N} e\left(Y_\tau^{(i)}\right)\ V_\tau^{(i)},$$

where $e(\cdot) = (e_1(\cdot), \ldots, e_M(\cdot))'$ and $A^{(M,N)} = \left[\frac{1}{N}\sum_{i=1}^{N} e_k(Y_\tau^{(i)})\,e_l(Y_\tau^{(i)})\right]_{1\le k,l\le M}$ is invertible for large enough N since we assume that the basis functions are linearly independent. Hence:

$$\hat{\alpha}^{(N)} \to \alpha = (\alpha_1, \ldots, \alpha_M)' = \left(A^{(M)}\right)^{-1} \mathbb{E}^{\tilde{\mathbb{P}}}\left[e\left(Y_\tau\right)\ \left(\sum_{k=\tau}^{T} x_k\right)\right]\ \tilde{\mathbb{P}}\text{-a.s.},$$

by the law of large numbers, where $A^M = \left[\mathbb{E}^{\tilde{\mathbb{P}}}\left[e_k\left(Y_\tau\right)\, e_l\left(Y_\tau\right)\right]\right]_{1\le k,l\le M}$, so that:

$$\widehat{C}_\tau^{(M,N)} = e'\,\hat{\alpha}^{(N)} \to e'\alpha = \widehat{C}_\tau^{(M)}\ \tilde{\mathbb{P}}\text{-a.s.}$$

Finally, for the third part, write:

$$V_\tau^{(i)} = \sum_{k=\tau}^{T} x_k\left(Y_\tau^{(i)}\right) = \sum_{j=1}^{M} \alpha_j e_j\left(Y_\tau^{(i)}\right) + \epsilon_j,$$

where $\mathbb{E}\left[\epsilon_j|Y_\tau\right] = 0, \mathrm{Var}\left[\epsilon_j|Y_\tau\right] = \Sigma(Y_\tau)$, and $\mathrm{Cov}\left[\epsilon_i,\, \epsilon_j|Y_\tau\right] = 0$. Thus (see e.g. Section 6.13 in Amemiya (1985)):

$$\sqrt{N}[\alpha - \hat{\alpha}^{(N)}] \longrightarrow \text{Normal}\left[0, \underbrace{\left(A^{(M)}\right)^{-1}\left[\mathbb{E}^{\mathbb{P}}\left[e_k(Y_\tau)e_l(Y_\tau)\Sigma(Y_\tau)\right]\right]_{1\le k,\,l\le M}\left(A^{(M)}\right)^{-1}}_{\tilde{\xi}}\right],$$

so that:

$$\sqrt{N}\left[\widehat{C}_\tau^{(M)} - \widehat{C}_\tau^{(M,N)}\right] = e'[\alpha - \hat{\alpha}^{(N)}]\sqrt{N} \longrightarrow \text{Normal}\ (0, \xi^{(M)}),$$

where:

$$\xi^{(M)} = e'\,\tilde{\xi}\,e. \tag{23}$$

□

Proof of Corollary 3.1. Relying on the notation from the proof of Proposition 3.1, we now have:

$$\hat{\alpha}^{(N)} = \frac{1}{N}\sum_{i=1}^{N} e\left(Y_\tau^{(i)}\right)\, V_\tau^{(i)} \to \alpha,\ N \to \infty$$

in $L^2(\Omega, \mathcal{F}, \tilde{\mathbb{P}})$ by the L^2-version of the weak law of large numbers (Durett, 1996). Thus:

$$\begin{aligned}
\mathbb{E}^{\tilde{\mathbb{P}}}\left[\left|e(Y_\tau)'\,\hat{\alpha}^{(N)} - e(Y_\tau)'\,\alpha\right|\right] &\le \sum_{k=1}^{M} \mathbb{E}^{\tilde{\mathbb{P}}}\left[\left|e_k(Y_\tau)'\,\left(\hat{\alpha}_k^{(N)} - \alpha_k\right)\right|\right] \\
&\le \sum_{k=1}^{M} \sqrt{\mathbb{E}^{\tilde{\mathbb{P}}}\left[e_k^2(Y_\tau)\right]}\sqrt{\mathbb{E}^{\tilde{\mathbb{P}}}\left[\hat{\alpha}_k^{(N)} - \alpha_k\right]^2} \to 0,\ N \to \infty.
\end{aligned}$$

The last assertion in the statement is a direct consequence of the Extended Namioka Theorem in Biagini and Fritelli (2009). □

Proof of Proposition 3.2. Since $(V_\tau^{(i)}, Y_\tau^{(i)})$ are i.i.d. as Monte Carlo trials, the first part of Assumption 1 in Newey (1997) is automatically satisfied. The conditions in the proposition are then exactly Assumptions 1 (part 2), 2, and 3 in his paper for $d = 0$. Thus, the claim follows by the first part of Theorem 1 in Newey (1997). □

Proof of Proposition 3.3. Analogously to the proof of Proposition 3.2, the first part of Assumption 1 in Newey (1997) is automatically satisfied. The conditions in the proposition are taken from the second part of Assumption 1, Assumption 8, the discussion following Assumption 8, and Assumption 9 in his paper. Thus, the claim follows by the first part of Theorem 4 in Newey (1997). □

Proof of Corollary 3.2. The first assertion immediately follows from convergence in distribution as discussed in Section 3.1. For the quantiles, the convergence for all continuity points of $F_{C_\tau}^{-1}$ follows from Proposition 3.1 and the standard proof of Skorokhod's representation theorem (see e.g. Lemma 1.7 in Whitt (2002)). □

Regularity Conditions in Proposition 3.4 (Gordy and Juneja, 2010). Regularity conditions on the joint probability function (pdf) g of $(-\widehat{C}_\tau^{(M)}, Z^{(N)})$:

- The joint pdf $g_N(\cdot,\cdot)$, its partial derivatives $\frac{\partial}{\partial y} g_N(y,z)$, and $\frac{\partial^2}{\partial y^2} g_N(y,z)$ exist for each N and for all (y,z).
- For $N \geq 1$, there exist non-negative functions $p_{0,N}(\cdot)$, $p_{1,N}(\cdot)$, and $p_{2,N}(\cdot)$ such that:
  - $g_N(y,z) \leq p_{0,N}(z)$,
  - $\left|\frac{\partial}{\partial y} g_N(y,z)\right| \leq p_{1,N}(z)$,
  - $\left|\frac{\partial^2}{\partial y^2} g_N(y,z)\right| \leq p_{2,N}(z)$, and

  for all y and z. In addition:

$$\sup_N \int_{-\infty}^{\infty} |z|^r p_{i,N}(z) dz < \infty$$

  for $i = 0, 1, 2$ and $0 \leq r \leq 4$.

The proof of Proposition 3.4 directly follows Proposition 2 in Gordy and Juneja (2010). □

Singular Value Decomposition of a Compact Operator (Section 4.2). Suppose the operator A mapping from $\mathcal{H}_1$ to $\mathcal{H}_2$ is compact, where $\mathcal{H}_1$ and $\mathcal{H}_2$ are separable Hilbert spaces. Then, A can be represented in the following form (see Section VI.3 in Werner (2005) or Huang (2012)):

$$A\mathbf{x} = \sum_{k=1}^{\infty} \lambda_k \langle \mathbf{x}, g_k \rangle_{\mathcal{H}_1} f_k, \tag{24}$$

where:

- $\langle \cdot, \cdot \rangle_{\mathcal{H}_1}$ denotes the inner product in $\mathcal{H}_1$;
- $\{\lambda_k^2\}$ are non-zero eigenvalues of A^*A and AA^* with $\lambda_1 \geq \lambda_2 \geq \cdots$, counted according to their multiplicity. Here, λ_k is called the k-th singular value of A;

- $\{g_k\} \subset \mathcal{H}_1$, called the (right) *singular functions*, are the orthonormal eigenfunctions of A^*A; and
- $\{f_k\} \subset \mathcal{H}_2$, called the (left) *singular functions*, are the orthonormal eigenfunctions of AA^* satisfying $A\, g_k = \lambda_k\, f_k$.

The representation (24) is called *singular value decomposition* (SVD) of A and the triple (λ_k, g_k, f_k) is called *singular system* for A. The functional sequences, $\{g_k\}_{k\geq 1}$ and $\{f_k\}_{k\geq 1}$, form complete orthonormal sequences of $\mathcal{H}_1$ and $\mathcal{H}_2$, respectively. The singular values λ_k are non-negative and the only possible accumulation point is zero. □

Proof of Proposition 4.1. We consider the approximation of L by an arbitrary rank-M operator L_F, which can be represented as:

$$L_F = \sum_{k=1}^{M} \alpha_k \langle \cdot\,, u_k \rangle\, e_k,$$

where $\{\alpha_k\}_{k=1}^M \subseteq \mathbb{R}_+$, $\{u_k\}_{k=1}^M$ are orthonormal in $\mathcal{H}$, and $\{e_k\}_{k=1}^M$ are orthonormal in $L^2\left(\mathbb{R}^d, \mathcal{B}, \mathbb{P}_{Y_\tau}\right)$. Denote by L_F^* the operator when choosing $(\alpha_k, u_k, e_k) = (\omega_k, s_k, \varphi_k)$. Then:

$$\begin{aligned}
\inf_{L_F} \|L - L_F\|^2 &\leq \sup_{\|\mathbf{x}\|=1} \|L\mathbf{x} - L_F^*\mathbf{x}\|^2 \\
&= \sup_{\|\mathbf{x}\|=1} \left\| \sum_{k=M+1}^{\infty} \omega_k \langle \mathbf{x}, s_k \rangle \varphi_j \right\|^2 \\
&= \sup_{\|\mathbf{x}\|=1} \sum_{k=M+1}^{\infty} \omega_k^2 \langle \mathbf{x}, s_k \rangle^2 \;=\; \omega_{M+1}^2.
\end{aligned}$$

On the other hand, consider any alternative system (α_k, u_k, e_k) for an arbitrary finite-rank operator L_F. Then choose a non-zero $\mathbf{x}_0$ such that $\mathbf{x}_0 \in \text{lin}\{s_1, ..., s_{M+1}\} \cap \text{lin}\{u_1, ..., u_M\}^\perp \neq \{0\}$. Note that $L - L_F$ is compact and bounded. Therefore:

$$\begin{aligned}
\|L - L_F\|^2 \geq \frac{\|L\mathbf{x}_0 - L_F\,\mathbf{x}_0\|^2}{\|\mathbf{x}_0\|^2} &= \frac{\|L\mathbf{x}_0\|^2}{\|\mathbf{x}_0\|^2} \\
= \frac{\sum_{k=1}^{M+1} \omega_k^2 |\langle \mathbf{x}_0, s_k \rangle|^2}{\sum_{k=1}^{M+1} |\langle \mathbf{x}_0, s_k \rangle|^2} &\geq \omega_{M+1}^2.
\end{aligned}$$

Hence:

$$\inf_{L_F} \|L - L_F\|^2 = \omega_{M+1}^2 = \|L - L_F^*\|.$$

Now since:

$$\inf_{L_F} \|L - L_F\|^2 = \inf_{\{e_1,...,e_M\}} \|L - P(e_1, ..., e_M) \cdot\, L\|^2,$$

where $P(e_1, ..., e_M)$ denotes the orthogonal projection on the subspace spanned by $(e_1, ..., e_M)$, the claim follows by Equation (7). □

Proof of Proposition 4.2. Proceeding as in Equation (9) and with Equation (7), we obtain:

$$\begin{aligned}\inf_{\alpha_M}\sup_{y\in\mathcal{Y}}\left|C_\tau(y)-\sum_{k=1}^{M}\alpha_{M,k}\,e_k(y)\right| &\leq \sup_{y\in\mathcal{Y}}\left|C_\tau(y)-\widehat{C}_\tau^{(M)}(y)\right| \\ &= \sup_{y\in\mathcal{Y}}\Big|\sum_{k=M+1}^{\infty}\omega_k\,\langle \mathbf{x},s_k\rangle\,\varphi_k(y)\Big| \\ &\leq \sum_{k=M+1}^{\infty}\omega_k\,|\langle \mathbf{x},s_k\rangle|\,\sup_{y\in\mathcal{Y}}|\varphi_k(y)| \\ &\leq \sum_{k=M+1}^{\infty}\omega_k\,\|\mathbf{x}\|\,\|s_k\|\,\sup_{y\in\mathcal{Y}}|\varphi_k(y)| \\ &= \sum_{k=M+1}^{\infty}\omega_k\,\|\mathbf{x}\|\,\sup_{y\in\mathcal{Y}}|\varphi_k(y)| = O\left(\omega_M\right)\end{aligned}$$

for a fixed $\mathbf{x}$ since the $\{\varphi_k\}$ are uniformly bounded, where the second and third inequalities follow by the triangle and Cauchy-Schwarz inequalities, respectively.

Then, going through the assumptions of Proposition 3.2 with $B=I$ and $e^{(M)}=(e_1,...,e_M)'$, we obtain:

$$\mathbb{E}^{\tilde{\mathbb{P}}}\left[\tilde{e}^{(M)}(Y_\tau)\tilde{e}^{(M)}(Y_\tau)'\right]=I$$

due to the orthonormality of the singular functions. Therefore, the smallest eigenvalues is bounded away from zero uniformly for every M. Moreover, for fixed $y\in\mathcal{Y}$, $||\tilde{e}^{(M)}(y)||=\sqrt{\varphi_1(y)^2+\cdots\varphi_M(y)^2}$, so that:

$$\begin{aligned}\sup_{y\in\mathcal{Y}}||\tilde{e}^{(M)}(y)|| =& \sup_{y\in\mathcal{Y}}\sqrt{\varphi_1(y)^2+\cdots\varphi_1(y)^2} \\ \leq& \sqrt{\sum_{k=1}^{M}\sup_{y\in\mathcal{Y}}\varphi_k(y)^2} \leq \sqrt{\max_{1\leq k\leq M}\sup_{y\in\mathcal{Y}}\varphi_k(y)\cdot M}=C\sqrt{M}=\zeta_0(M)\end{aligned}$$

since the $\{\varphi_k\}$ are uniformly bounded. Thus, the claim follows by Proposition 3.2. □

Proof of Lemma 4.1. The assertions on the conditional distributions are standard. For showing that L is compact, we check that the transition and the reverse transition density functions satisfy the condition in Lemma 2.3. Note that the transition density function can be written as:

$$\begin{aligned}\pi_{Y_T|Y_\tau}(y|x) &= g(y;\mu_T+\Gamma'\Sigma_\tau^{-1}(x-\mu_\tau),\Sigma_{T|\tau}) \\ &= \frac{1}{(2\pi)^{d/2}|\Sigma_{T|\tau}|^{1/2}}\exp\left[-\frac{1}{2}\left(y-\mu_T-\Gamma'\Sigma_\tau^{-1}(x-\mu_\tau)\right)'\Sigma_{T|\tau}^{-1}\left(y-\mu_T-\Gamma'\Sigma_\tau^{-1}(x-\mu_\tau)\right)\right] \\ &= \frac{1}{(2\pi)^{d/2}|\Sigma_{T|\tau}|^{1/2}}\frac{\left|\Sigma_\tau(\Gamma')^{-1}\Sigma_{T|\tau}\Gamma^{-1}\Sigma_\tau\right|^{1/2}}{\left|\Sigma_\tau(\Gamma')^{-1}\Sigma_{T|\tau}\Gamma^{-1}\Sigma_\tau\right|^{1/2}} \\ &\quad\times\exp\left[-\frac{1}{2}\left(x-\mu_\tau-\Sigma_\tau(\Gamma')^{-1}(y-\mu_T)\right)'\Sigma_\tau^{-1}\Gamma\Sigma_{T|\tau}^{-1}\Gamma'\Sigma_\tau^{-1}\left(x-\mu_\tau-\Sigma_\tau(\Gamma')^{-1}(y-\mu_T)\right)\right] \\ &= \frac{|\Sigma_\tau|}{|\Gamma|}g\left(x;\mu_\tau+\Sigma_\tau(\Gamma')^{-1}(y-\mu_T),\Sigma_\tau(\Gamma')^{-1}\Sigma_{T|\tau}\Gamma^{-1}\Sigma_\tau\right).\end{aligned}$$

We evaluate the following integral:

$$
\begin{aligned}
&\int_{\mathbb{R}^d} \pi_{Y_T|Y_\tau}(y|x)\pi_{Y_\tau|Y_T}(x|y)dx \\
&= \frac{|\Sigma_\tau|}{|\Gamma|}\int_{\mathbb{R}^d} g\left(x;\mu_\tau+\Sigma_\tau(\Gamma')^{-1}(y-\mu_T),\Sigma_\tau(\Gamma')^{-1}\Sigma_{T|\tau}\Gamma^{-1}\Sigma_\tau\right) \\
&\qquad\qquad \times g\left(x;\mu_\tau+\Gamma\Sigma_\tau^{-1}(y-\mu_T),\Sigma_{\tau|T}\right)\,dx \\
&= \frac{|\Sigma_\tau|}{|\Gamma|(2\pi)^{d/2}}\frac{1}{\left|\Sigma_\tau(\Gamma')^{-1}\Sigma_{T|\tau}\Gamma^{-1}\Sigma_\tau+\Sigma_{\tau|T}\right|^{1/2}} \\
&\quad \times \exp\Bigg[-\frac{1}{2}\left(\Sigma_\tau(\Gamma')^{-1}(y-\mu_T)-\Gamma\Sigma_T^{-1}(y-\mu_T)\right)'\left(\Sigma_\tau(\Gamma')^{-1}\Sigma_{T|\tau}\Gamma^{-1}\Sigma_\tau+\Sigma_{\tau|T}\right)^{-1} \\
&\qquad\qquad \times\left(\Sigma_\tau(\Gamma')^{-1}(y-\mu_T)-\Gamma\Sigma_T^{-1}(y-\mu_T)\right)\Bigg] \\
&= \frac{|\Sigma_\tau|}{|\Gamma|(2\pi)^{d/2}}\frac{1}{\left|\Sigma_\tau(\Gamma')^{-1}\Sigma_{T|\tau}\Gamma^{-1}\Sigma_\tau+\Sigma_{\tau|T}\right|^{1/2}} \\
&\quad \times \exp\Bigg[-\frac{1}{2}(y-\mu_T)'\underbrace{\left(\Gamma^{-1}\Sigma_\tau-\Sigma_T^{-1}\Gamma'\right)\left(\Sigma_\tau(\Gamma')^{-1}\Sigma_{T|\tau}\Gamma^{-1}\Sigma_\tau+\Sigma_{\tau|T}\right)^{-1}\left(\Sigma_\tau(\Gamma')^{-1}-\Gamma\Sigma_T^{-1}\right)}_{V^{-1}}(y-\mu_T)\Bigg] \\
&= C_1\times g(y;\mu_T,V),
\end{aligned}
$$

where we use results on the product of Gaussian densities (Vinga, 2004) and where C_1 is an appropriate constant to obtain $g(y;\mu_T,V)$. Therefore:

$$
\int_{\mathbb{R}^d}\int_{\mathbb{R}^d}\pi_{Y_T|Y_\tau}(y|x)\pi_{Y_\tau|Y_T}(x|y)\,dx\,dy=\int_{\mathbb{R}^d}C_1 g(y;\mu_T,V)\,dy=C_1<\infty.
$$

□

Proof of Lemma 4.2. L^* can be found via:

$$
\begin{aligned}
\langle Lh,m\rangle_{\pi_{Y_\tau}} &= \int_{\mathbb{R}^d} Lh(x)\,m(x)\,\pi_{Y_\tau}(x)\,dx=\int_{\mathbb{R}^d}\left[\int_{\mathbb{R}^d}h(y)\pi_{Y_T|Y_\tau}(y|x)\,dy\right]m(x)\,\pi_{Y_\tau}(x)\,dx \\
&= \int_{\mathbb{R}^d}h(y)\left[\int_{\mathbb{R}^d}m(x)\pi_{Y_\tau|Y_T}(x|y)\,dx\right]\pi_{Y_T}(y)\,dy=\langle h,L^*m\rangle_{\pi_{Y_T}},
\end{aligned}
$$

where $L^*m(y)=\int_{\mathbb{R}^d}m(x)\pi_{Y_\tau|Y_T}(x|y)\,dx$. We obtain for LL^*:

$$
\begin{aligned}
LL^*\varphi(x) &= \int_{\mathbb{R}^d}L^*\varphi(s)\pi_{Y_T|Y_\tau}(s|x)\,ds \\
&= \int_{\mathbb{R}^d}\left[\int_{\mathbb{R}^d}\varphi(y)\pi_{Y_\tau|Y_T}(y|s)\,dy\right]\pi_{Y_T|Y_\tau}(s|x)\,ds \\
&= \int_{\mathbb{R}^d}\varphi(y)\underbrace{\int_{\mathbb{R}^d}\pi_{Y_\tau|Y_T}(y|s)\pi_{Y_T|Y_\tau}(s|x)\,ds}_{K_A(x,y)}\,dy.
\end{aligned}
$$

It is useful to express the reverse density as in the proof of Lemma 4.1:

$$g(y;\mu_{Y_\tau|s},\Sigma_{\tau|T}) = \frac{|\Sigma_T|}{|\Gamma|} g\left(s;\mu_T+\Sigma_T\Gamma^{-1}(y-\mu_\tau),\ \Sigma_T\Gamma^{-1}\Sigma_{\tau|T}(\Gamma')^{-1}\Sigma_T\right).$$

Hence:

$$\begin{aligned}
K_A(x,y) &= \int_{\mathbb{R}^d} \pi_{Y_\tau|Y_T}(y|s)\pi_{Y_T|Y_\tau}(s|x)\,ds \\
&= \frac{|\Sigma_T|}{|\Gamma|}\int_{\mathbb{R}^d} g\left(s;\mu_T+\Sigma_T\Gamma^{-1}(y-\mu_\tau),\ \Sigma_T\Gamma^{-1}\Sigma_{\tau|T}(\Gamma')^{-1}\Sigma_T]\right)\times g(s;\mu_{T|x},\Sigma_{T|\tau})\,ds \\
&= \frac{|\Sigma_T|}{|\Gamma|}\times\frac{1}{(2\pi)^{d/2}\left|\Sigma_T\Gamma^{-1}\Sigma_{\tau|T}(\Gamma')^{-1}\Sigma_T+\Sigma_{T|\tau}\right|^{1/2}} \\
&\quad\times\exp\Bigg(-\frac{1}{2}\left(\Sigma_T\Gamma^{-1}(y-\mu_\tau)-\Gamma'\Sigma_\tau^{-1}(x-\mu_\tau)\right)' \\
&\qquad\times\left(\Sigma_T\Gamma^{-1}\Sigma_{\tau|T}(\Gamma')^{-1}\Sigma_T+\Sigma_{T|\tau}\right)^{-1}\left(\Sigma_T\Gamma^{-1}(y-\mu_\tau)-\Gamma'\Sigma_\tau^{-1}(x-\mu_\tau)\right)\Bigg) \\
&= \frac{1}{(2\pi)^{d/2}\left|\Gamma\Sigma_T^{-1}\left(\Sigma_T\Gamma^{-1}\Sigma_{\tau|T}(\Gamma')^{-1}\Sigma_T+\Sigma_{T|\tau}\right)\Sigma_T^{-1}\Gamma'\right|^{1/2}} \\
&\quad\times\exp\Bigg(-\frac{1}{2}\left(y-\mu_\tau-\Gamma\Sigma_T^{-1}\Gamma'\Sigma_\tau^{-1}(x-\mu_\tau)\right)'(\Gamma^{-1})'\Sigma_T\left(\Sigma_T\Gamma^{-1}\Sigma_{\tau|T}(\Gamma')^{-1}\Sigma_T+\Sigma_{T|\tau}\right)^{-1} \\
&\qquad\times\Sigma_T\Gamma^{-1}\left(y-\mu_\tau-\Gamma\Sigma_T^{-1}\Gamma'\Sigma_\tau^{-1}(x-\mu_\tau)\right)\Bigg) \\
&= g\big(y;\mu_\tau+\underbrace{\Gamma\Sigma_T^{-1}\Gamma'\Sigma_\tau^{-1}}_{A}(x-\mu_\tau),\ \Sigma_\tau-\Gamma\Sigma_T^{-1}\Gamma'\Sigma_\tau^{-1}\Gamma\Sigma_T^{-1}\Gamma'\big) \\
&= g\big(y;\underbrace{\mu_\tau+A(x-\mu_\tau)}_{\mu_A(x)},\ \underbrace{\Sigma_\tau-A\Sigma_\tau A'}_{\Sigma_A}\big) = g\big(y;\mu_A(x),\Sigma_A\big),
\end{aligned}$$

where in the third equality we again rely on results on the products of Gaussian densities from Vinga (2004). L^*L can be derived analogously. □

Proof of Lemma 4.3. We start by recalling the considerations from Khare and Zhou (2009): Let (X_t) on $\mathbb{R}^d$ be a MAR(1) process satisfying the following stochastic difference equation:

$$X_t = \Phi X_{t-1}+\eta_t,\quad t\geq 1, \tag{25}$$

where $\Phi\in\mathbb{R}^{d\times d}$ and $(\eta_t)_{t\geq 1}$ are independent and identically distributed, $\eta_1\sim N(0,H)$. (X_t) has a unique stationary distribution $N(0,\Sigma)$ if and only if $H=\Sigma-\Phi\Sigma\Phi'$, and the process is reversible if and only if $\Phi\Sigma=\Sigma\Phi'$. Khare and Zhou (2009) show that if these assumptions are satisfied, the transformed Markov operator for (25) has eigenvalues which are products of eigenvalues of Φ and the corresponding eigenfunctions are products of Hermite polynomials.

Now note that for a random variable Y that is distributed according to $K_A(x,\cdot)$, we can write:

$$Y-\mu_\tau = A(x-\mu_\tau)+\zeta_A, \tag{26}$$

where $\zeta\sim N(0,\Sigma_A)$. Since from Lemma 4.2 we have that $\Sigma_A=\Sigma_\tau-A\Sigma_\tau A'$ and:

$$A\Sigma_\tau = \Gamma\Sigma_T^{-1}\Gamma' = \Sigma_\tau\,A',$$

for $\Sigma = \Sigma_\tau$ the operator $L\,L^*$ has the same structure of the Markov operator for (25) that is reversible and stationary.

Following the approach by Khare and Zhou (2009), denote by $\Sigma_\tau^{1/2}$ the square root matrix of Σ_τ. Then:

$$\Sigma_\tau^{-1/2} A \Sigma_\tau^{1/2} = \Sigma_\tau^{-1/2}\,\Gamma \Sigma_T^{-1} \Gamma' \Sigma_\tau^{-1/2}$$

is symmetric and thus orthogonally diagonalizable:

$$\Sigma_\tau^{-1/2} A \Sigma_\tau^{1/2} = P \Lambda P' \;\Leftrightarrow\; A = (\Sigma_\tau^{1/2}\,P)\,\Lambda\,(P' \Sigma_\tau^{-1/2}).$$

In particular, the entries of the diagonal matrix Λ are the eigenvalues of A.

Now for the transformation (11) of the random vector Y from (26), $z^P(Y)$, we obtain:

$$\begin{aligned}\mathbb{E}_{K_A}\left[z^P(Y)|x\right] &= P'\Sigma_\tau^{-1/2} A (x - \mu_\tau) \\ &= P'\Sigma_\tau^{-1/2}\Sigma_\tau^{1/2} P \Lambda P' \Sigma_\tau^{-1/2}(x - \mu_\tau) = \Lambda z^P(x),\end{aligned}$$

and:

$$\begin{aligned}\mathrm{Var}_{K_A}\left[z^P(Y)|x\right] &= P'\Sigma_\tau^{-1/2}\Sigma_A \Sigma_\tau^{-1/2} P \\ &= P'\Sigma_\tau^{-1/2}(\Sigma_\tau - A\Sigma_\tau A')\Sigma_\tau^{-1/2} P = I - \Lambda^2.\end{aligned}$$

Moreover:

$$\mathbb{E}_{\pi_{Y_\tau}}\left[z^P(Y_\tau)\right] = P'\Sigma_\tau^{-1/2}\mathbb{E}_{\pi_{Y_\tau}}\left[Y_\tau - \mu_\tau\right] = 0$$

and:

$$\mathrm{Var}_{\pi_{Y_\tau}}\left[z^P(Y_\tau)\right] = P'\Sigma_\tau^{-1/2}\Sigma_\tau\Sigma_\tau^{-1/2} P = I.$$

The second part follows analogously. □

Proof of Proposition 4.3. For fixed $z_i^P(Y)$, we obtain from Carrasco and Florens (2011) that the univariate orthonormal Hermite polynomial of order n_i is an eigenfunction under K_A :

$$\mathbb{E}_{K_A}\left[h_{n_i}(z_i^P(Y))|x\right] = \lambda_i^{n_i} h_{n_i}(z_i^P(x)).$$

Moreover, the product of these polynomials are also eigenfunction since:

$$\mathbb{E}_{K_A}\left[\Pi_{i=1}^d h_{n_i}(z_i^P(Y))|x\right] = \Pi_{i=1}^d \mathbb{E}_{K_A}\left[h_{n_i}(z_i^P(Y))|x\right] = \left(\Pi_{i=1}^d \lambda_i^{n_i}\right)\left(\Pi_{i=1}^d h_{n_i}(z_i^P(x))\right).$$

The orthogonality of the eigenfunctions is proved in Khare and Zhou (2009). Note that the product of normalized Hermite polynomials is already normalized since:

$$\mathbb{E}_{\pi_{Y_\tau}}\left[\left(\Pi_{i=1}^d h_{n_i}(z_i^P(Y))\right)^2\right] = \mathbb{E}_{\pi_{Y_\tau}}\left[\Pi_{i=1}^d h_{n_i}\left(z_i^P\right)^2(Y)\right] = \Pi_{i=1}^d \mathbb{E}_{\pi_{Y_\tau}}\left[h_{n_i}\left(z_i^P(Y)\right)^2\right] = 1.$$

Right singular functions are obtained similarly from $z_i^Q(X)$. □

Proof of Lemma 5.1. Under $\mathbb{P}$, the solutions of (15), (16), and (17) at time τ are:

$$\begin{aligned} q_\tau &= q_0 + \left(m - \frac{1}{2}\sigma_S^2\right)\tau + \sigma_S \int_0^\tau dW_s^S, \\ r_\tau &= r_0 e^{-\alpha\tau} + \gamma\left(1 - e^{-\alpha\tau}\right) + \sigma_r \int_0^\tau e^{-\alpha(\tau-t)} dW_t^r, \\ \mu_{x+\tau} &= \mu_x e^{\kappa\tau} + \psi \int_0^\tau e^{\kappa(\tau-u)} dW_u^\mu. \end{aligned}$$

Thus, the joint Gaussian distribution of Y_τ is given by:

$$\begin{bmatrix} q_\tau \\ r_\tau \\ \mu_{x+\tau} \end{bmatrix} \sim N\left(\begin{bmatrix} q_0 + \left(m - \frac{1}{2}\sigma_S^2\right)\tau \\ r_0 e^{-\alpha\tau} + \gamma\left(1 - e^{-\alpha\tau}\right) \\ \mu_x e^{\kappa\tau} \end{bmatrix}, \begin{bmatrix} \sigma_S^2\,\tau & \rho_{12}\sigma_S\sigma_r B_r(0,\tau) & \rho_{13}\sigma_S\psi B_\mu(0,\tau) \\ \rho_{12}\sigma_S\sigma_r B_r(0,\tau) & \sigma_r^2 \frac{1-e^{-2\alpha\tau}}{2\alpha} & \rho_{23}\sigma_r\psi \frac{1-e^{-(\alpha-\kappa)\tau}}{\alpha-\kappa} \\ \rho_{13}\sigma_S\psi B_\mu(0,\tau) & \rho_{23}\sigma_r\psi \frac{1-e^{-(\alpha-\kappa)\tau}}{\alpha-\kappa} & \psi^2 \frac{e^{2\kappa\tau}-1}{2\kappa} \end{bmatrix} \right), \tag{27}$$

so that μ_τ and Σ_τ are given by

$$\mu_\tau = \begin{bmatrix} q_0 + \left(m - \frac{1}{2}\sigma_S^2\right)\tau \\ r_0 e^{-\alpha\tau} + \gamma\left(1 - e^{-\alpha\tau}\right) \\ \mu_x e^{\kappa\tau} \end{bmatrix}, \quad \Sigma_\tau = \begin{bmatrix} \sigma_S^2\,\tau & \rho_{12}\sigma_S\sigma_r B_r(0,\tau) & \rho_{13}\sigma_S\psi B_\mu(0,\tau) \\ \rho_{12}\sigma_S\sigma_r B_r(0,\tau) & \sigma_r^2 \frac{1-e^{-2\alpha\tau}}{2\alpha} & \rho_{23}\sigma_r\psi \frac{1-e^{-(\alpha-\kappa)\tau}}{\alpha-\kappa} \\ \rho_{13}\sigma_S\psi B_\mu(0,\tau) & \rho_{23}\sigma_r\psi \frac{1-e^{-(\alpha-\kappa)\tau}}{\alpha-\kappa} & \psi^2 \frac{e^{2\kappa\tau}-1}{2\kappa} \end{bmatrix}.$$

To derive the distribution under $\mathbb{Q}_E$, first note that for $\tau \le s < T$:

$$\begin{aligned} r_s =& e^{-\alpha(s-\tau)} r_\tau + \left(\bar{\gamma} - \frac{\sigma_r^2}{\alpha^2}\right)\left(1 - e^{-\alpha(s-\tau)}\right) + \frac{\sigma_r^2}{2\alpha^2}\left(e^{-\alpha(T-s)} - e^{-\alpha(T+s-2\tau)}\right) \\ & - \frac{\rho_{23}\sigma_r\psi}{\kappa}\left(\frac{e^{\kappa(T-s)} - e^{-\alpha(s-\tau)+\kappa(T-\tau)}}{\alpha-\kappa} - \frac{1 - e^{-\alpha(s-\tau)}}{\alpha}\right) + \sigma_r \int_\tau^s e^{-\alpha(s-y)} dZ_y^r, \end{aligned}$$

so that the integral of $\int_\tau^T r_s\, ds$ can be evaluated using the stochastic Fubini theorem:

$$\begin{aligned} \int_\tau^T r_s ds =& \left(\frac{1 - e^{-\alpha(T-\tau)}}{\alpha}\right) r_\tau + \left(\bar{\gamma} - \frac{\sigma_r^2}{\alpha^2}\right)\left(T - \tau - \frac{1 - e^{-\alpha(T-\tau)}}{\alpha}\right) \\ & + \frac{\sigma_r^2}{2\alpha^2}\left(\frac{1 - e^{-\alpha(T-\tau)}}{\alpha} - \frac{e^{-\alpha(T-\tau)} - e^{-2\alpha(T-\tau)}}{\alpha}\right) \\ & - \frac{\rho_{23}\sigma_r\psi}{\kappa}\left(\frac{e^{\kappa(T-\tau)} - 1}{\kappa(\alpha-\kappa)} - \frac{e^{\kappa(T-\tau)} - e^{-(\alpha-\kappa)(T-\tau)}}{\alpha(\alpha-\kappa)} - \frac{1}{\alpha}\left(T - \tau - \frac{1 - e^{-\alpha(T-\tau)}}{\alpha}\right)\right) \\ & + \sigma_r \int_\tau^T \frac{1 - e^{-\alpha(T-y)}}{\alpha} dZ_y^r. \end{aligned}$$

Thus, under $\mathbb{Q}_E$ with known Y_τ, the solutions of (20), (21), and (22) are:

$$\begin{aligned}
q_T =& q_\tau + \left(\frac{1-e^{-\alpha(T-\tau)}}{\alpha}\right) r_\tau + \left(\bar{\gamma} - \frac{\sigma_r^2}{\alpha^2}\right)\left(T-\tau-\frac{1-e^{-\alpha(T-\tau)}}{\alpha}\right) \\
&+ \frac{\sigma_r^2}{2\alpha^2}\left(\frac{1-e^{-\alpha(T-\tau)}}{\alpha} - \frac{e^{-\alpha(T-\tau)}-e^{-2\alpha(T-\tau)}}{\alpha}\right) \\
&- \frac{1}{2}\sigma_S^2(T-\tau) - \frac{\rho_{12}\sigma_S\sigma_r}{\alpha}\left(T-\tau-\frac{1-e^{-\alpha(T-\tau)}}{\alpha}\right) - \frac{\rho_{13}\sigma_S\psi}{\kappa}\left(\frac{e^{\kappa(T-\tau)}-1}{\kappa} - T + \tau\right) \\
&- \frac{\rho_{23}\sigma_r\psi}{\kappa}\left(\frac{e^{\kappa(T-\tau)}-1}{\kappa(\alpha-\kappa)} - \frac{e^{\kappa(T-\tau)}-e^{-(\alpha-\kappa)(T-\tau)}}{\alpha(\alpha-\kappa)} - \frac{1}{\alpha}\left(T-\tau-\frac{1-e^{-\alpha(T-\tau)}}{\alpha}\right)\right) \\
&+ \sigma_S\int_\tau^T dZ_s^S + \sigma_r\int_\tau^T \frac{1-e^{-\alpha(T-y)}}{\alpha} dZ_y^r, \\
r_T =& e^{-\alpha(T-\tau)} r_\tau + \left(\bar{\gamma} - \frac{\sigma_r^2}{\alpha^2}\right)\left(1-e^{-\alpha(T-\tau)}\right) + \frac{\sigma_r^2}{2\alpha^2}\left(1-e^{-2\alpha(T-\tau)}\right) \\
&- \frac{\rho_{23}\sigma_r\psi}{\kappa}\left(\frac{1-e^{-(\alpha-\kappa)(T-\tau)}}{\alpha-\kappa} - \frac{1-e^{-\alpha(T-\tau)}}{\alpha}\right) + \sigma_r\int_\tau^T e^{-\alpha(T-y)} dZ_y^r, \\
\mu_{x+T} =& e^{\kappa(T-\tau)}\mu_{x+\tau} - \frac{\psi^2}{\kappa}\left(\frac{e^{2\kappa(T-\tau)}-1}{2\kappa} - \frac{e^{\kappa(T-\tau)}-1}{\kappa}\right) - \frac{\rho_{23}\sigma_r\psi}{\alpha}\left(\frac{e^{\kappa(T-\tau)}-1}{\kappa} - \frac{1-e^{-(\alpha-\kappa)(T-\tau)}}{\alpha-\kappa}\right) \\
&+ \psi\int_\tau^T e^{\kappa(T-t)} dZ_t^\mu,
\end{aligned}$$

so that the (Gaussian) conditional distribution of $Y_T|Y_\tau$ is given by:

$$\begin{pmatrix} q_T \\ r_T \\ \mu_{x+T} \end{pmatrix} |Y_\tau \sim N\left(\begin{bmatrix} \mu_{q_T|q_\tau} \\ \mu_{r_T|r_\tau} \\ \mu_{\mu_{x+T}|\mu_{x+\tau}} \end{bmatrix}, \underbrace{\begin{bmatrix} \sigma^2_{q_T|q_\tau} & \sigma_{q_T,r_T|q_\tau,r_\tau} & \sigma_{q_T,\mu_{x+T}|q_\tau,\mu_{x+\tau}} \\ \sigma_{q_T,r_T|q_\tau,r_\tau} & \sigma^2_{r_T|r_\tau} & \sigma_{r_T,\mu_{x+T}|r_\tau,\mu_{x+\tau}} \\ \sigma_{q_T,\mu_{x+T}|q_\tau,\mu_{x+\tau}} & \sigma_{r_T,\mu_{x+T}|r_\tau,\mu_{x+\tau}} & \sigma^2_{\mu_{x+T}|\mu_{x+\tau}} \end{bmatrix}}_{\Sigma_{T|\tau}} \right), \tag{28}$$

where:

$$\begin{aligned}
\mu_{q_T|q_\tau} =& q_\tau + B_r(\tau,T) r_\tau + \left(\bar{\gamma} - \frac{\sigma_r^2}{\alpha^2}\right)\left(T-\tau-\frac{1-e^{-\alpha(T-\tau)}}{\alpha}\right) \\
&+ \frac{\sigma_r^2}{2\alpha^2}\left(\frac{1-e^{-\alpha(T-\tau)}}{\alpha} - \frac{e^{-\alpha(T-\tau)}-e^{-2\alpha(T-\tau)}}{\alpha}\right) \\
&- \frac{\rho_{23}\sigma_r\psi}{\kappa}\left(\frac{e^{\kappa(T-\tau)}-1}{\kappa(\alpha-\kappa)} - \frac{e^{\kappa(T-\tau)}-e^{-(\alpha-\kappa)(T-\tau)}}{\alpha(\alpha-\kappa)} - \frac{1}{\alpha}\left(T-\tau-\frac{1-e^{-\alpha(T-\tau)}}{\alpha}\right)\right) \\
&- \frac{1}{2}\sigma_S^2(T-\tau) - \frac{\rho_{12}\sigma_S\sigma_r}{\alpha}\left(T-\tau-\frac{1-e^{-\alpha(T-\tau)}}{\alpha}\right) - \frac{\rho_{13}\sigma_S\psi}{\kappa}\left(\frac{e^{\kappa(T-\tau)}-1}{\kappa} - T + \tau\right),
\end{aligned}$$

$$
\begin{aligned}
\mu_{r_T|r_\tau} =& e^{-\alpha(T-\tau)} r_\tau + \left(\bar{\gamma} - \frac{\sigma_r^2}{\alpha^2}\right)\left(1 - e^{-\alpha(T-\tau)}\right) + \frac{\sigma_r^2}{2\alpha^2}\left(1 - e^{-2\alpha(T-\tau)}\right) \\
& - \frac{\rho_{23}\sigma_r\psi}{\kappa}\left(\frac{1 - e^{-(\alpha-\kappa)(T-\tau)}}{\alpha - \kappa} - \frac{1 - e^{-\alpha(T-\tau)}}{\alpha}\right), \\
\mu_{\mu_{x+T}|\mu_{x+\tau}} =& \mu_{x+\tau} e^{\kappa(T-\tau)} - \frac{\rho_{23}\sigma_r\psi}{\alpha}\left(\frac{e^{\kappa(T-\tau)} - 1}{\kappa} - \frac{1 - e^{-(\alpha-\kappa)(T-\tau)}}{\alpha - \kappa}\right) \\
& - \frac{\psi^2}{\kappa}\left(\frac{e^{2\kappa(T-\tau)} - 1}{2\kappa} - \frac{e^{\kappa(T-\tau)} - 1}{\kappa}\right), \\
\sigma^2_{q_T|q_\tau} =& \sigma_S^2 (T-\tau) + \frac{\sigma_r^2}{\alpha^2}\left(T - \tau - 2\frac{1 - e^{-\alpha(T-\tau)}}{\alpha} + \frac{1 - e^{-2\alpha(T-\tau)}}{2\alpha}\right) \\
& + \frac{2\rho_{12}\sigma_S\sigma_r}{\alpha}\left(T - \tau - \frac{1 - e^{-\alpha(T-\tau)}}{\alpha}\right), \\
\sigma_{q_T, r_T|q_\tau, r_\tau} =& \rho_{12}\sigma_S\sigma_r\left(\frac{1 - e^{-\alpha(T-\tau)}}{\alpha}\right) + \frac{\sigma_r^2}{\alpha}\left(\frac{1 - 2e^{-\alpha(T-\tau)} + e^{-2\alpha(T-\tau)}}{2\alpha}\right), \\
\sigma_{q_T, \mu_{x+T}|q_\tau, \mu_{x+\tau}} =& \rho_{13}\sigma_S\psi\left(\frac{e^{\kappa(T-\tau)} - 1}{\kappa}\right) + \frac{\rho_{23}\sigma_r\psi}{\alpha}\left(\frac{e^{\kappa(T-\tau)} - 1}{\kappa} - \frac{1 - e^{-(\alpha-\kappa)(T-\tau)}}{\alpha - \kappa}\right), \\
\sigma^2_{r_T|r_\tau} =& \sigma_r^2\left(\frac{1 - e^{-2\alpha(T-\tau)}}{2\alpha}\right), \\
\sigma_{r_T, \mu_{x+T}|r_\tau, \mu_{x+\tau}} =& \rho_{23}\sigma_r\psi\left(\frac{1 - e^{-(\alpha-\kappa)(T-\tau)}}{\alpha - \kappa}\right), \\
\sigma^2_{\mu_{x+T}|\mu_{x+\tau}} =& \psi^2\left(\frac{e^{2\kappa(T-\tau)} - 1}{2\kappa}\right).
\end{aligned}
$$

It is possible to write the conditional mean of Y_T given Y_τ in the following affine form:

$$
\begin{aligned}
\begin{bmatrix} \mu_{q_T|q_\tau} \\ \mu_{r_T|r_\tau} \\ \mu_{\mu_{x+T}|\mu_{x+\tau}} \end{bmatrix} =& \underbrace{\begin{bmatrix} 1 & \frac{1-e^{-\alpha(T-\tau)}}{\alpha} & 0 \\ 0 & e^{-\alpha(T-\tau)} & 0 \\ 0 & 0 & e^{\kappa(T-\tau)} \end{bmatrix}}_{H} \begin{bmatrix} q_\tau \\ r_\tau \\ \mu_{x+\tau} \end{bmatrix} + C_\tau \\
=& HY_\tau + C_\tau,
\end{aligned}
$$

where C_τ is a constant matrix defined by remaining terms of mean vector of $Y_T|Y_\tau$ after defining HY_τ. The unconditional distribution of Y_T under $\tilde{\mathbb{P}}$ is also Gaussian since Y_τ and $Y_T|Y_\tau$ follow Gaussian distributions. Thus, it suffices to specify a mean vector and a covariance matrix of Y_T under $\tilde{\mathbb{P}}$ to specify its distribution:

$$
\begin{aligned}
\mu_T = \mathbb{E}^{\tilde{\mathbb{P}}}[Y_T] &= \mathbb{E}^{\mathbb{P}}\left[\mathbb{E}^{\mathbb{Q}_E}[Y_T|Y_\tau]\right] = \mathbb{E}^{\mathbb{P}}\left[HY_\tau + C_\tau\right] = H\mu_\tau + C_\tau, \\
\Sigma_T = \mathrm{Cov}^{\tilde{\mathbb{P}}}[Y_T] &= \mathrm{Cov}^{\mathbb{P}}\left[\mathbb{E}^{\mathbb{Q}_E}[Y_T|Y_\tau]\right] + \mathbb{E}^{\mathbb{P}}\left[\mathrm{Cov}^{\mathbb{Q}_E}[Y_T|Y_\tau]\right] \\
&= \mathrm{Cov}^{\mathbb{P}}\left[HY_\tau + C_\tau\right] + \mathbb{E}^{\mathbb{P}}\left[\Sigma_{T|\tau}\right] = H\Sigma_\tau H' + \Sigma_{T|\tau}.
\end{aligned}
$$

Hence, $Y_T \sim N(\mu_T,\ \Sigma_T)$.

The final step is to specify the joint distribution of Y_τ and Y_T by finding $\mathrm{Cov}(Y_\tau, Y_T)$. Note that:

$$\begin{aligned}\Gamma = \mathrm{Cov}(Y_\tau, Y_T) &= \mathbb{E}^{\tilde{\mathbb{P}}}[Y_\tau Y_T'] - \mathbb{E}^{\tilde{\mathbb{P}}}[Y_\tau]\mathbb{E}^{\tilde{\mathbb{P}}}[Y_T'] \\ &= \mathbb{E}^{\mathbb{P}}[\mathbb{E}^{\mathbb{Q}_E}[Y_\tau Y_T'|Y_\tau]] - \mu_\tau \mu_T' \\ &= \mathbb{E}^{\mathbb{P}}\left[Y_\tau(Y_\tau' H' + C_\tau')\right] - \mu_\tau \mu_T' \\ &= \Sigma_\tau H'.\end{aligned}$$

Therefore,

$$\begin{bmatrix} Y_\tau \\ Y_T \end{bmatrix} \sim N\left(\begin{bmatrix} \mu_\tau \\ \mu_T \end{bmatrix}, \quad \begin{bmatrix} \Sigma_\tau & \Gamma \\ \Gamma' & \Sigma_T \end{bmatrix}\right).$$

□

References

Amemiya, T., 1985. Advanced econometrics. Harvard university press, Cambridge.

Biagini, F., Frittelli, M., 2009. On the extension of the Namioka-Klee theorem and on the Fatou property of risk measures. In Optimality and risk: modern trends in mathematical finance – The Kebanov Festschrift (Eds. F. Delbaen, M. Rasonyi, and Ch. Stricker), 1-29.

Carrasco M., Florens J., 2011. Spectral Method for Deconvolving a Density. Econometric Theory, 27: 546-581.

Durett, R., 1996. Probability: theory and examples, Second Edition. Duxbury Press, Belmont, CA.

Gordy, M.B., Juneja, D., 2010. Nested simulations in portfolio risk measurement. Management Science, 56: 1833-1848.

Huang, Q., 2012. Some Topics Concerning the Singular Value Decomposition and Generalized Singular Value Decomposition. Ph.D. thesis, Arizona State University.

Khare, K., Zhou, H., 2009. Rate of Convergence of Some Multivariate Markov Chains with Polynomial Eigenfunctions. The Annals of Applied Probability, 19: 737-777.

Newey, W.K., 1997. Convergence rates and asymptotic normality for series estimators. Journal of Econometrics, 79: 147-168.

Vinga, S., 2004. Supplementary material to Vinga, S., Almeida, J.S., 2004. Rényi continuous entropy of DNA sequences. Journal of Theoretical Biology 231: 377-388.

Werner, D., 2005. Funktionalanalysis, Fifth Edition. Springer, Berlin.

Whitt, W., 2002. Internet Supplement to "Stochastic-Process Limits" (Springer Series in Operations Research, 2002). Available at `http://www.columbia.edu/~ww2040/`.